AD-A137 805 STUDY OF NOISE-CERTIFICATION STANDARDS FOR AIRCRAFT ENGINES VOLUME 3 SELE..(U) DYTEC ENGINEERING INC LONG BEACH CA A H MARSH ET AL. DEC 83 FAA/EE-82-11-VOL-3 1/1

UNCLASSIFIED DOT-FA78WA-4096 F/G 21/5 NL

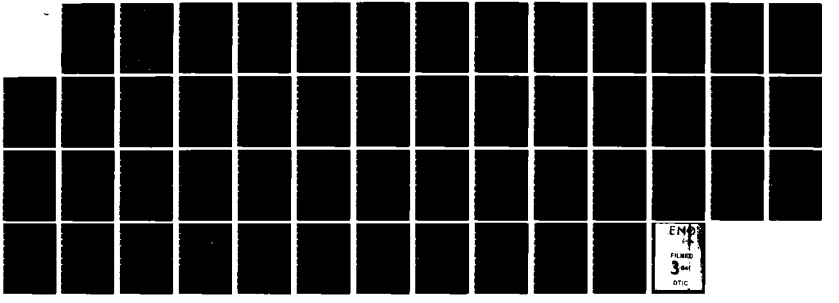

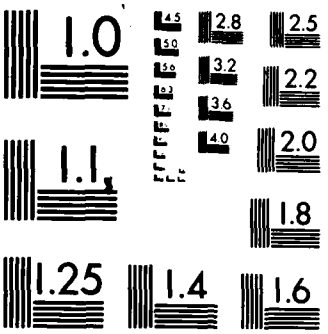

MICROCOPY RESOLUTION TEST CHART
NATIONAL BUREAU OF STANDARDS-1963-A

FAA/EE-82-11, Volume 3

Office of Environment
and Energy
Washington, D.C. 20591

(12)

Study of Noise-Certification Standards for Aircraft Engines

Volume 3: Selection and Evaluation of Engine-Noise-Certification Concept

Alan H. Marsh, Robert L. Chapkis*,
and Gary L. Blankenship†

DyTec Engineering, Inc.
5092 Tasman Drive
Huntington Beach, CA 92649

(*now at Douglas Aircraft Company
Long Beach, CA 90646)

(†now at Gulfstream Aerospace
Savannah, GA 31402)

December 1983

Final Report

U.S. Department of Transportation
Federal Aviation Administration

NOTICE

Technical Report Documentation Page

1. Report No.	2. Government Accession No.	3. Recipient's Catalog No.
FAA-EE-82-11, Vol. 3	AD-A137 805	

4. Title and Subtitle	5. Report Date
Study of Noise-Certification Standards for Aircraft Engines Volume 3: Selection and Evaluation of Engine-Noise-Certification Concept	December 1983
	6. Performing Organization Code 7906
7. Author(s) Alan H. Marsh, Robert L. Chapkis*, and Gary L. Blankenship†	8. Performing Organization Report No.
9. Performing Organization Name and Address DyTec Engineering, Inc. 5092 Tasman Drive Huntington Beach, CA 92649	10. Work Unit No. (TRAIS)
	11. Contract or Grant No. DOT-FA78WA-4096
12. Sponsoring Agency Name and Address U.S. Department of Transportation Federal Aviation Administration Office of Environment and Energy Washington, DC 20591	13. Type of Report and Period Covered Final Report
	14. Sponsoring Agency Code

15. Supplementary Notes

Now with:
*Douglas Aircraft Company, Long Beach, CA 90846
†Gulfstream Aerospace, Savannah, GA 31402

16. Abstract

This study, reported in three volumes, had the purpose of considering the feasibility of establishing an FAA requirement for a manufacturer of aircraft engines to demonstrate compliance with an engine noise-level standard in order to obtain an engine-noise type certificate. The objective of engine-noise type certification (if feasible on the basis of economic reasonableness, technological practicality, and appropriateness to the type design) would be to supplement the aircraft-noise type certification requirements in Part 36 of the Federal Aviation Regulations. The scope of the study was limited to aircraft jet engines.

Volume 3 describes the selection of a concept for the noise-evaluation quantity, namely the A-frequency-weighted sound power made nondimensional by a power-like quantity equal to the product of total net static thrust and the speed of sound in the ambient air. The recommended independent variable is total net static thrust made nondimensional by the product of total mass flow rate and the speed of sound in the ambient air. Farfield 1/3-octave-band sound pressure levels, measured around production and experimental versions of aircraft turbojet and turbofan engines, were used to test the utility and applicability of the recommended noise-evaluation quantity. The engines ranged in rated static thrust from 11 kN to 222 kN (2500 lb to 50,000 lb). For certification purposes, a certifying authority would select appropriate limits on the magnitude of the noise-evaluation quantity applicable to thrust settings representative of takeoff and landing approach.

17. Key Words	18. Distribution Statement
Engine-noise type certification Turbofan engines Aircraft-engine noise control Static engine-noise testing	Availability unlimited. Report is available to the public through the National Technical Information Service, Springfield, VA 22161

19. Security Classif. (of this report)	20. Security Classif. (of this page)	21. No. of Pages	22. Price
Unclassified	Unclassified	52	

Form DOT F 1700.7 (8-72) Reproduction of completed page authorized

METRIC CONVERSION FACTORS

Approximate Conversions to Metric Measures

Symbol	When You Know	Multiply by	To Find	Symbol
	LENGTH			
in	inches	*2.5	centimeters	cm
ft	feet	30	centimeters	cm
yd	yards	0.9	meters	m
mi	miles	1.6	kilometers	km
	AREA			
in^2	square inches	6.5	square centimeters	cm^2
ft^2	square feet	0.09	square meters	m^2
yd^2	square yards	0.8	square meters	m^2
mi^2	square miles	2.6	square kilometers	km^2
	acres	0.4	hectares	ha
	MASS (weight)			
oz	ounces	28	grams	g
lb	pounds	0.45	kilograms	kg
	short tons (2000 lb)	0.9	tonnes	t
	VOLUME			
tsp	teaspoons	5	milliliters	ml
Tbsp	tablespoons	15	milliliters	ml
fl oz	fluid ounces	30	milliliters	ml
c	cups	0.24	liters	l
pt	pints	0.47	liters	l
qt	quarts	0.95	liters	l
gal	gallons	3.8	liters	l
ft^3	cubic feet	0.03	cubic meters	m^3
yd^3	cubic yards	0.76	cubic meters	m^3
	TEMPERATURE (exact)			
°F	Fahrenheit temperature	5/9 (after subtracting 32)	Celsius temperature	°C

*1 in = 2.54 (exactly). For other exact conversions and more detailed tables, see NBS Misc. Publ. 286, Units of Weights and Measures, Price $2.25, SD Catalog No. C13.10:286.

Approximate Conversions from Metric Measures

Symbol	When You Know	Multiply by	To Find	Symbol
	LENGTH			
mm	millimeters	0.04	inches	in
cm	centimeters	0.4	inches	in
m	meters	3.3	feet	ft
m	meters	1.1	yards	yd
km	kilometers	0.6	miles	mi
	AREA			
cm^2	square centimeters	0.16	square inches	in^2
m^2	square meters	1.2	square yards	yd^2
km^2	square kilometers	0.4	square miles	mi^2
ha	hectares (10,000 m^2)	2.5	acres	
	MASS (weight)			
g	grams	0.035	ounces	oz
kg	kilograms	2.2	pounds	lb
t	tonnes (1000 kg)	1.1	short tons	
	VOLUME			
ml	milliliters	0.03	fluid ounces	fl oz
l	liters	2.1	pints	pt
l	liters	1.06	quarts	qt
l	liters	0.26	gallons	gal
m^3	cubic meters	35	cubic feet	ft^3
m^3	cubic meters	1.3	cubic yards	yd^3
	TEMPERATURE (exact)			
°C	Celsius temperature	9/5 (then add 32)	Fahrenheit temperature	°F

CONTENTS

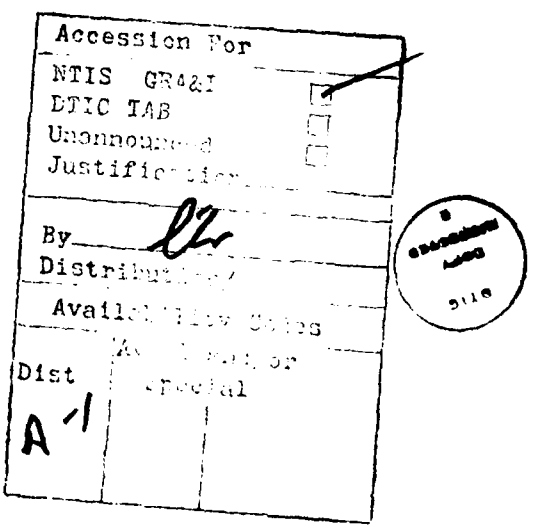

TABLES

ILLUSTRATIONS

ACKNOWLEDGMENTS

It is a pleasure to acknowledge the cooperation of the engine manufacturers, the NASA Lewis Research Center, and the USAF Aerospace Medical Research Laboratory in supplying a large part of the acoustical and engine-performance data used for the analyses presented in this report.

STUDY OF NOISE-CERTIFICATION STANDARDS FOR AIRCRAFT ENGINES

VOLUME 3: SELECTION AND EVALUATION OF ENGINE-NOISE-CERTIFICATION CONCEPT

INTRODUCTION

This report is the third in a three-volume series that presents results of a study of the feasibility of establishing federal standards to limit the level of noise produced by jet engines. If issued, the standards would be part of a requirement for an engine manufacturer to obtain a noise type certificate for an engine in addition to the basic engine airworthiness type certificate. The Introduction of Volume 1 provides additional background information on the study, [1][1].

Volume 2 contains a discussion of procedures for the measurement of farfield sound pressure levels and presents specific recommendations for conducting static-engine tests, analyzing the measurements, and reporting the results, [2].

The subject of this report is the selection and evaluation of a concept for use as the noise-level standard in a requirement for certification of the noise produced by an engine of a given type. Sound pressure levels are assumed to be measured and analyzed in accordance with the recommendations in Volume 2.

The next section describes the selection of the noise-evaluation quantity and its use as a concept for static-engine noise certification. We then describe the engines for which farfield noise data and accompanying engine-performance data were obtained. The final two main sections of the report describe the method used to analyze the test data and the results of applying the method to the various sets of measured noise levels.

It was concluded that it would be technically feasible to evaluate the noise produced by an engine on a test stand for the purpose of engine-noise certification. The noise-certification concept based on nondimensional A-frequency-weighted sound power and nondimensional total static thrust is shown to provide a meaningful rating of the noise produced by a large variety of jet engines as well as the noise reduction achieved by various noise-control measures.

A cost-benefit analysis to evaluate the economic reasonableness and assess the appropriateness of a requirement for static-engine noise certification was not within the scope of the study reported here. Such an analysis would have required detailed economic data from the engine and airplane manufacturers as well as estimates of the impact on noise levels in communities around airports as a consequence of the establishment of a requirement for engine noise certification in conjunction with the continuing requirements in FAR Part 36 for certification of airplane noise.

---

[1]Bracketed numbers refer to documents listed in the References Section.

NOISE CERTIFICATION CONCEPT

This Section describes the various noise-evaluation quantities that were examined and discusses the rationale for selection of nondimensional A-frequency-weighted sound power as the noise-evaluation quantity of choice. Selection of appropriate limits for the noise-evaluation quantity would be a consensus procedure and was not within the scope of the study reported here.

Considerations in the selection of the noise-evaluation quantity were:

- the quantity should have just one possible value at any given engine power setting;
- the quantity should be sensitive enough to properly indicate the effect of incorporating noise-control design features within the basic engine;
- the quantity should not be so different from the quantity used for aircraft noise certification [i.e., effective perceived noise level and its components perceived noise level and tone-corrected perceived noise level] that an engine manufacturer would have to incorporate special noise-control design features which would not also help to reduce the effective perceived noise from an airplane on which the engine might be installed;
- the quantity should include a frequency weighting so that changes in engine design to incorporate various noise-control features could be expected to be reasonably evaluated in terms of corresponding changes in community response; and
- the quantity should be readily computed by standard techniques.

Consistent with the recommendations in Ref. 2, it was also considered that the noise-evaluation quantity should be computed from equivalent free-field sound pressure levels, i.e., sound pressure levels free of ground-reflection effects including spectral distortions caused by phase differences between direct and reflected sound waves. Thus, the free-field conditions are those of an anechoic space, not those of a free-field above a perfectly reflecting plane [i.e., a hemi-anechoic space].

The sound pressure levels used to compute the noise-evaluation quantity should be adjusted for differences between the atmospheric absorption that was present under test-day conditions and that which would exist under acoustical-reference-day conditions.

For reasons enumerated in Ref. 2, the configuration of the test engine was not to simulate an inlet or exhaust ducts as installed on an airplane. Therefore, it was considered that the noise-evaluation quantity should not include any attempt to account for the unique effects associated with various installations of an engine on an airplane.

Omission of engine-installation effects from the noise-evaluation quantity was not considered to be a serious detriment because the objectives outlined above should still be achievable without significant impact on the applicability of the noise-evaluation quantity for certification of engine noise.

On the other hand, consideration of forward-motion effects was regarded as a potentially important element for the noise-evaluation quantity. It was known that forward motion alters both the directivity as well as the acoustic power produced by the various sources of sound from turbofan (or turbojet) engines. In an attempt to develop a method to account for forward-motion effects, we reviewed various analytical and empirical procedures. For reference, the Appendix lists the reports that were reviewed as part of the effort to develop a procedure for quantifying the effects of forward motion on noise measured around an engine on a test stand.

The review of the literature on forward-motion effects led to the conclusion not to attempt to incorporate any forward-motion effect in the noise-evaluation quantity.

That decision was based on two principal considerations:

(1) the state-of-the-art at the time was such that reliable, validated procedures applicable to all relevant engine noise sources were not available for the various types and installations of existing turbofan engines; and

(2) the forward-motion adjustments would have to be applied to the sound pressure levels produced by each relevant source of engine noise and no data were available to establish source noise levels for a variety of engines.

Thus, it was decided not to incorporate either engine-installation or forward-motion effects. The noise-evaluation quantity was to be based on equivalent free-field sound pressure levels in the acoustic farfield around an engine on a test stand. The engine would be equipped with hardwall reference inlet and exhaust ducts. All noise-control features that are part of the design for the basic engine would be installed.

Having made the decisions described above, there were several alternatives available for the choice of the noise-evaluation quantity. One choice was the maximum value of a frequency-weighted quantity along a geometric path such as an arc of a circle centered on the engine reference point or along a line to the side of the engine and parallel to the engine centerline. Microphones have been located on polar or sideline arrays for many engine noise tests. The frequency-weighted quantity could be perceived noise level, tone-corrected perceived noise level, or A-frequency-weighted sound level where the perceived noisiness and A-frequency weighting are given in national (and international) standards.

The radial distance to the polar arc or the lateral distance to the sideline array would need to be specified, but the distance should not be much greater than the distance at the time of the tests in order to avoid the introduction of ambiguities during the extrapolation process, especially for extended noise sources such as jet noise.

Furthermore, the distance could not be a constant (e.g., 50 meters) because a distance suitable for a small engine would likely place the microphones too close to a large engine, and vice versa.

The choice of a noise-evaluation quantity based solely on a maximum value was, however, rejected because small changes in engine configuration or atmospheric condition could produce significant changes in directivity and thus alter the magnitude of the maximum value. The reproducibility of a measurement of the maximum value of a noise-evaluation quantity would have to be established before such a concept could be adopted.

Thus, after considering several options, it was decided to base the noise-evaluation quantity on a surface-and-time-average measure of the noise produced by an engine, namely the sound power radiated into the farfield.

The reasons for adopting a measure based on averaging over the area of a closed surface surrounding the engine as well as averaging over a period of time included:

- averaging over the area of a surface for noise levels measured a[illegible]d a static engine is comparable to the integration over time for no[illegible] levels measured by a microphone near the ground from an airplane flyin[illegible]head;
- sound power levels, in particular A-weighted sound power levels, are widely used for rating the noise produced by stationary machinery;
- standard procedures are available in national and international documents for computing the sound power level produced by a noise source on a reflecting plane [3, 4];
- except for atmospheric-absorption effects, sound power level is not a function of distance from the source and hence should be appropriate for large as well as small engines; and
- the acoustic power produced by a jet engine should be a function of the fundamental physical processes by which the fan and the compressor, combustor, and turbine components add mechanical and thermal energy to the flow of air through the engine to produce useful work in the form of propulsive thrust.

The last of the reasons given above for adopting acoustic power as the fundamental component of the noise-evaluation measure was considered to be particularly important because, as shown by Heidmann and Feiler [5] and by McCune and Kerrebrock [6], the acoustic power radiated into the farfield by a jet engine is proportional to the work done on the air flowing through the engine and hence is proportional to the net propulsive thrust.

The fundamental relation between an engine's acoustic power output and the net propulsive thrust thus provided a quantity which should be applicable to a wide range of turbofan (or turbojet) engines.

In addition, if the net thrust is multiplied by a velocity then the product is a power-like term which can be utilized to form a nondimensional ratio with acoustic power. A nondimensional ratio avoids confusion that could arise from the use of various units for the numerator and denominator terms [e.g., watts per newton, kilowatts per lb, and so on]*

*The nondimensional power ratio is a refinement to the concept based on A-weighted sound power level that was described in the Appendix of Ref. 2.

Because the sound pressure levels used to calculate the sound power levels would be adjusted for differences in atmospheric absorption under test-time and reference meteorological conditions, the quantity chosen for a velocity was the speed of sound at the reference temperature of 25° C, i.e., approximately 346 m/s.

The parameter of acoustic power per unit of total net thrust was considered to be a fundamental measure capable of correlating the sound from a variety of engines. Thrust forces are routinely measured by most engine test stands used for acoustical tests. Thus, the selected parameters for the noise-evaluation quantity can be measured by practical instruments and also permit physically meaningful interpretations.

The frequency weighting provided by the standard A-weighting is close enough to the frequency weighting for perceived noisiness that design features incorporated to reduce farfield perceived noise levels should yield comparable reductions in A-weighted sound power levels. Thus, A-weighted sound power level should be able to satisfy all the requirements for a noise-evaluation quantity stated at the beginning of this Section.

With W_A as the letter symbol for A-weighted sound power in watts, F_n for net thrust in newtons, and c_∞ for the speed of sound in meters/second, the nondimensional form for the noise-evaluation quantity may be expressed in symbols as $W_A/F_n c_\infty$.

However, because the A-weighted sound power in the numerator will always be much less than the power term in the denominator, the standard reference sound power W_{ref} of one picowatt (1 pW = 10^{-12} watts) was introduced to provide values for the nondimensional ratio that are greater than unity Introduction of the standard reference sound power also permitted the usage of sound power levels as commonly calculated with the decibel as the unit.

Convenient and positive values in decibels for the nondimensional power ratio on a logarithmic scale were obtained by introducing a reference mechanical power, Π_{ref}, into the denominator. A value of one watt was chosen for Π_{ref}.

Thus,

$$10 \lg[(W_A/W_{ref})/(F_n c_\infty/\Pi_{ref})] = 10 \lg(W_A/W_{ref}) - 10 \lg(F_n c_\infty/\Pi_{ref}) \quad (1)$$

$$= L_{WA} - 10 \lg(F_n c_\infty/\Pi_{ref}) \quad (2)$$

where L_{WA} is the standard letter symbol for A-weighted sound power level.

Equation (1) may also be written as

$$10 \lg[(W_A/W_{ref})/(F_n c_\infty/\Pi_{ref})] = 10 \lg(W_A/F_n c_\infty) + 10 \lg(\Pi_{ref}/W_{ref}) \quad (3)$$

or, alternatively, as

$$10 \lg[(W_A/W_{ref})/(F_n c_\infty/\Pi_{ref})] = 10 \lg(W_A/F_n c_\infty) + 120 \quad (4)$$

by substituting the values for W_{ref} and Π_{ref}.

For the experimental and production versions of the jet engines for which data were available, the value of the A-weighted noise-evaluation quantity, by Eqs. (1) to (4), ranged from approximately 65 dB to 90 dB. That 35-dB range included thrusts from takeoff-rated thrust to approximately 20 percent of takeoff thrust and a wide range of noise-control design features. Detailed results are presented in a subsequent Section.

The parameter chosen for the independent variable to correlate the data, and to provide a means of relating the noise-evaluation quantity to engine power setting, was the nondimensional ratio of the total measured net static thrust to a thrust-like term. The thrust-like term was the product of the measured mass flow rate, $\dot{M}$, of air through the engine and the reference speed of sound, c_∞.

In symbols, the independent variable for use with the recommended noise-evaluation quantity was $F_n/\dot{M}c_\infty$ where net thrust, F_n, has the newton as the unit if mass flow rate $\dot{M}$ has the unit of kilograms/second and the speed of sound c_∞ has meters/second as the unit. For the jet engines included in the study, the nondimensional net thrust ranged from approximately 0.3 to 1.5 over a range of engine power settings.

Note that since c_∞ is a constant, the ratio $F_n/\dot{M}$ is essentially equal to the specific thrust or thrust per unit mass flow rate, i.e., an effective velocity. Thus, the nondimensional thrust ratio is also a Mach number relative to a reference speed of sound. The mass flow of the fuel was neglected because it is small compared with the mass flow of air.

ENGINES AND NOISE DATA

Assessment of the ability of the recommended noise-evaluation quantity to correlate noise levels produced by various engines required the identification, acquisition, evaluation, and processing of measured farfield sound pressure levels. This Section describes the sources of engine noise data that were examined and gives the characteristics of the fifteen engines for which data were ultimately included in the study.

Most of the existing measurements of engine noise were acquired by the engine manufacturers and were regarded as proprietary information. However, some data were available in the public domain as a result of studies funded by government agencies. In addition, some data were acquired from engine manufacturers solely for use in this study, but with the understanding that details of the data would remain proprietary.

The types of engines included turbojets as well as turbofans in order to provide information on a limiting case (i.e., bypass ratio zero) as well as high exhaust velocities. Military as well as commercial engines were included to expand the size of the data base. Data for one turbojet engine (the Olympus 593) included an afterburning [reheat] condition as well as maximum static thrust without afterburning.

The two turbojet engines were production versions of actual engines. The thirteen turbofan engines included nine production engines and four experimental engines. Sound pressure levels measured around the experimental engines also provided information on the ability of the noise-evaluation quantity to assess

the noise reduction associated with different noise-control measures incorporated within the basic engine or in an inlet or exhaust duct.

References 7 to 18 were the sources for the sound pressure level data for the fifteen engines included in the study. References 19 to 29 contain additional data that may be useful for future studies.

Table 1 lists the characteristics of the eleven production engines and the configurations of the inlet and exhaust ducts as they were for the tests for which sound pressure level data were available.

Note that, although the engines listed in Table 1 are all production engines, the configuration of the inlet and exhaust ducts is not necessarily the same as used when the engine is installed on an airplane. The JT4A-3 was installed on DC-8 airplanes, for example, with an external mixer and a retractable ejector instead of the round, conical nozzle. Instead of hardwall inlet and exhaust ducts, the JT8D-15 is usually installed with sound-absorbing duct linings to reduce fan noise. Similarly, the JT8D-209 is installed on McDonnell Douglas MD-80 airplanes with an inlet that has sound-absorbing linings on the duct wall.

Table 2 describes the test configurations of the four experimental engines. For each engine, the data in Refs. 15 to 18 provided sound pressure levels for various versions of the inlet duct, fan-exhaust duct, turbine-exhaust duct, or nozzles. In all, Table 2 lists 30 different test configurations: ten for the NASA/GE Engine A, thirteen for the NASA/GE Engine C, three for the NASA/P&WA JT8D-109 Refan, and four for the NASA/Lycoming YF-102 for the QSRA airplane. The design technology incorporated in the engines of Tables 1 and 2 spans a period of approximately 20 years from the mid 1950s to the mid 1970s. As shown later, the noise reduction achieved over that period of time is significant.

With the eleven configurations of production engines and the 30 test configurations of experimental engines, there was a total of 41 separate combinations of engines and test arrangments. For each of the 41, sound pressure levels were available for from one to eleven different power settings. At each engine power setting, there were one-third-octave-band sound pressure levels for the 24 bands with preferred frequencies from 50 Hz to 10,000 Hz, and sometimes for 30 bands from 25 Hz to 20,000 Hz. In addition, for each test, one-third-octave-band sound pressure levels were obtained from as many as 20 microphones.

The sum over all test runs of the product of the number of microphones per test run times the number of power settings per test run times the number of one-third octave bands represents the total number of sound pressure levels that had to be transcribed from tabulated data listings. That total was somewhat more than 68,000 individual 3-digit or 4-digit numbers to a precision of 0.1 decibel.

The task of processing the data was accomplished by a digital computer to produce the values of the noise-evaluation quantity for each data set. The next Section describes the analysis method incorporated in the computer program that was prepared to process the data.

Data selected for analysis were, in large part, measured around acoustical test facilities that met the minimal requirements given in the Appendix of Ref. 2. Moreoever, all data were checked for internal consistency. Some errors in the accompanying engine performance data were detected and revised data were obtained.

ANALYSIS METHOD

The sound power level from an engine at some power setting was computed from sound pressure levels measured at, or adjusted for inverse-square-distance to, locations along a circular array with a radius of 45.7 meters (150 feet). The locations were at engine centerline height above the ground plane. The sound pressure levels were assumed to be those that would be measured in hemianechoic space above a perfectly reflecting plane, i.e., 3 dB greater than would be measured in anechoic space.

The sound field was assumed to be rotationally symmetric about the engine's axis. The surface of the 45.7-m-radius hemisphere was divided into zones where the limiting angles defining the boundaries of the zones were those angles midway between the polar angles marking the locations of the microphones along the 45.7-m circular arc.

The sound power radiated out through each zone [in each of the 24 one-third-octave frequency bands] was computed from the product of the approximate time-average sound intensity and the surface area of the zone of the hemisphere. The approximate 1/3-octave-band sound intensity was computed from the farfield 1/3-octave-band sound pressure level by assuming that sound waves at the microphone were nearly plane or spherical waves and thus that farfield sound pressure levels (re 20 μPa) approximately equal farfield sound intensity levels (re 1 pW/m^2). The 1/3-octave-band sound powers through the various zones were summed to obtain the total sound power radiated through the hemisphere. Sound power levels were computed in decibels relative to the standard reference acoustic power of one picowatt (1 pW).

The A-frequency weighting was added to the 1/3-octave-band sound power levels to determine A-weighted, 1/3-octave-band sound power levels. The A-weighted sound power in each 1/3-octave frequency band from 50 Hz to 10,000 Hz was then summed to yield the wideband A-weighted sound power over that frequency range, i.e., the A-weighted sound power level, L_{WA}.

The total unweighted (or flat-weighted) sound power level, symbol L_{WT} with T for flaT, was also calculated from the sum of the unweighted 1/3-octave band sound powers.

As part of the effort under this study, a computer program was prepared to control the data-processing operations. To enhance the usefulness of the results, the computer program included a number of features in addition to the calculation of flat-weighted and A-weighted sound power levels.

The first step was to read in the input sound pressure levels and the accompanying values of atmospheric and engine power conditions associated with the input sound pressure levels. Because the input data were from diverse sources and had been measured around a variety of test stands using a variety of test pro-

cedures, it was necessary to account for the effects of those variables in order to adjust the input data to common reference conditions.

Some sound pressure levels were measured by microphones on poles or masts at the height of the engine centerline (or higher). Some sound pressure levels were measured by microphones located near (or on) the ground.

Since it had been decided to compute the sound power levels from sound pressure levels that could be regarded as equivalent to those measured in an acoustic free field above a reflecting plane, the ground-plane sound pressure levels were adjusted to be comparable, in an approximate way, to those which would have been measured by pole-mounted microphones at the same radius and angle relative to the engine reference point. The approximate adjustment consisted simply of a subtraction of 3 dB from the measured ground-plane 1/3-octave-band sound pressure levels.

Some of the input data were provided with adjustments already applied for differences between atmospheric absorption under test-time conditions and those for an acoustical reference day with an air temperature of 25° C and a relative humidity of 70 percent.

The atmospheric conditions for some of the input data were the as-measured test-time conditions. Some data had been adjusted to conditions of 15° C and 70-percent relative humidity.

For consistency, all input sound pressure levels were adjusted, if required, to the atmospheric absorption of an acoustical reference day. The method of SAE ARP 866A-1975 was used to determine coefficients of atmospheric absorption per unit distance.

Some input sound pressure levels were provided for locations along a sideline, some for locations along a circular arc. The radius of the arc varied from 30.5 m to 46.5 m. All input sound pressure levels were adjusted to locations along a circular arc with a radius of 45.7 m (150 ft). As a matter of interest, the data were also adjusted to represent measurements at the same polar angle, but on a 61-m sideline.

Distance adjustments utilized an inverse-square relationship for spherical wave divergence on the assumption that the microphones were in the farfield and all sources of engine noise could be considered as simple acoustic sources at the engine reference point.

Other than the 3-dB subtraction to approximately convert ground-microphone data to pole-microphone data, no adjustments were included to remove the spectral irregularities caused by ground-reflection interference effects. Spectral irregularities caused by differences between the phases of the sound waves impinging on the microphone were not removed for the follwoing reasons: (1) many measurements were made over a ground surface of dirt or irregular broken rock of unknown acoustic impedance, (2) most of the pole-mounted microphones were at a height such that the significant spectral irregularities were at relatively low frequencies (generally in the 1/3-octave bands having preferred frequencies less than 250 Hz), and (3) the effect of the A-frequency weighting reduces the contribution of the sound power in the low-frequency bands such that removal of low-frequency spectral irregularities would not have a large influence on the total A-weighted sound power level.

In addition, at high engine power settings, many engines produce relatively high levels of sound having a line spectrum with many harmonics of the fan rotational speed. That sound, often called multiple-pure-tone (MPT) or buzzsaw sound, is part of the sound produced by an engine and should be included in any measure of engine noise. Furthermore, the spectrum of MPT sound was believed to be unique to each specific engine of a given type because of unique fan-blade spacings and unique fan-blade shapes.

Any computational procedure for removing spectral irregularities caused by ground-reflection phase-interference effects must not also remove the real contributions of MPT sounds. An analytical (or combination of analytical and empirical) procedure capable of properly removing ground-reflection spectral irregularities from data measured around a variety of test stands, but not also removing actual MPT sounds, did not exist and was another reason why no attempts were made to remove spectral irregularities caused by ground-reflection effects.

Figures 1 to 5 present examples of running the computer program for one set of input data from a test of Engine C [item 11 in Table 2(b)].

Figure 1 shows the input data as 1/3-octave-band sound pressure levels at various angles relative to the inlet centerline and along a 46.5-m circular arc. The headings to the table give a description of the test configuration, the source of the data, test site, microphone installation method, engine design-point conditions, and various engine-performance and test conditions. Note that the ground surface between the engine and the microphones was crushed rock.

At the foot of the table are listings of calculated values of wideband, flat-weighted (overall) sound pressure level, A-weighted sound level, perceived noise level, tone-corrected perceived noise level and the magnitude of the largest tone correction. The band number for the 1/3-octave band sound pressure level that caused the largest tone correction is also tabulated at each angle. Band number 17 (50 Hz) is shown if the tone correction was zero.

To the left of the columns of 1/3-octave-band sound pressure levels are lists of the standard band numbers and the associated preferred frequencies from 50 hertz to 10,000 hertz. For correlation of the spectra with analytical studies, the third column from the left also gives the Strouhal number [STRHL NUMBR].

Strouhal number was calculated from fD/V where f was the preferred frequency, D was a characteristic dimension of the engine noise source, and V was the effective velocity of the jet exhaust.

Characteristic dimension D was taken as the equivalent diameter for the total exit area of the fan and primary nozzles, or 1.4 m in the example of Fig. 1.

Effective velocity V was taken as the ratio of total net thrust to inlet mass flow rate, or 268.1 m/s for the example of Fig. 1 for a net thrust of approximately 97,900 N and a total mass flow rate of 365.1 kg/s.

For Engine C at this highest test power setting, the Strouhal number ranged from 0.26 at 50 Hz to 52.2 at 10,000 Hz.

Figures 2 and 3 show data listings similar to the listings of input data in Fig. 1, but adjusted for acoustical reference-day atmospheric absorption. Figure 2 gives 1/3-octave-band sound pressure levels on a 61-m sideline. Figure 3 gives the sound pressure levels at the locations along the 45.7-m-radius arc.

Sound pressure levels on the 45.7-m arc were used to calculate sound power levels as follows.

In any frequency band, the sound intensity level, $L_I(j)$, at the j-th microphone is approximately equal to the sound pressure level, $L_p(j)$, that is

$$L_I(j) = 10 \lg(\bar{I}_j/I_{ref}) \approx L_p(j) \tag{5}$$

where $\bar{I}_j$ is the time average sound intensity and I_{ref} is the standard reference intensity.

From Eq. (5), the time-average sound intensity is given by

$$\bar{I}_j \approx (I_{ref})[10^{0.1L_p(j)}] \tag{6}$$

Sound power, W_j, radiated through area A_j of the j-th zone of a hemisphere around the engine is given by

$$W_j = \bar{I}_j A_j \tag{7}$$

where

$$A_j = \pi R^2(\cos \theta_j - \cos \theta_{j+1}) \tag{8}$$

for hemispherical radius R and zone boundary polar angles θ_j and θ_{j+1}.

The sound field is assumed to be rotationally symmetric about the engine's axis and thus $\bar{I}_j$ also represents the average sound intensity over zone area A_j.

The total sound power radiated through all zones is found from

$$W = \sum_j W_j \tag{9}$$

and the sound power level from

$$L_W = 10 \lg(W/W_{ref}) \tag{10}$$

The surface-average sound pressure level, $\langle L_p \rangle$, is found by considering the total sound power to be the product of the surface-average sound intensity, $\langle \bar{I} \rangle$, and the surface area, A_H, of the hemisphere. Thus,

$$W = \langle \bar{I} \rangle A_H \tag{11}$$

The sound power level may be expressed as

$$L_W = 10 \lg[(\langle \bar{I} \rangle A_H)/W_{ref}] \tag{12}$$

By analogy to Eq. (6),

$$\langle \bar{I} \rangle = (I_{ref})\left[10^{0.1\langle L_p \rangle}\right] \tag{13}$$

Combining Eqs. (12) and (13) yields

$$\begin{aligned} \langle L_p \rangle &= L_W - 10 \lg(I_{ref} A_H / W_{ref}) \\ &= L_W - 10 \lg(A_H / A_{ref}) \end{aligned} \tag{14}$$

where $A_{ref} = 1\ m^2$ if $I_{ref} = 10^{-12}\ W/m^2$ and $W_{ref} = 10^{-12}\ W$.

For a hemispherical radius of 45.7 m, the area term in Eq. (14) is 41.2 dB and Eq. (14) becomes

$$\langle L_p \rangle = L_W - 41.2 \tag{15}$$

For each 1/3-octave band, directivity indexes were calculated at each microphone angle along the 45.7-m-radius circular arc. Directivity index, *DI*, was found from

$$DI(j) = L_p(j) - \langle L_p \rangle \tag{16}$$

as the difference between the 1/3-octave-band sound pressure level and the corresponding surface-average sound pressure level.

Figure 4 presents the directivity indexes calculated from the sample test data. High-frequency sound pressure levels were most directional (i.e., had positive directivity indexes) in the forward quadrant from 10 degrees to 60 degrees. Low-frequency sound pressure levels were most directional in the aft quadrant from 110 degrees to 150 degrees.

Figure 5 lists the calculated values of flat-weighted and A-weighted sound power levels for each 1/3-octave band. Values for normalized 1/3-octave-band sound power levels, relative to the corresponding wideband sound power level, are also tabulated. For the example in Fig. 5, the peak of the flat-weighted and A-weighted sound power level spectra was in the 1/3-octave band at 500 Hz at a Strouhal number of 2.6.

Also listed in the data summary on Fig. 5 are: the surface-average 1/3-octave-band sound pressure levels and the sound pressure levels at the locations on the 61-m sideline of (1) maximum perceived noise level, (2) maximum tone-corrected perceived noise level, (3) maximum A-weighted sound level, and (4) maximum wideband flat-weighted, overall sound pressure level. For the example, all four quantities had their maximum value on the 61-m sideline at an angle of 70 degrees, as indicated at the foot of the table on the lower right.

The listings below the tabulated data in Fig. 5 give wideband flat-weighted and A-weighted sound power levels and wideband space-average sound pressure level.

Flat-weighted and A-weighted acoustic powers, in kilowatts, are tabulated as 1.021 kW and 0.603 kW for the example.

Jet-stream equivalent mechanical power was calculated from $(1/2)\dot{M}V^2 = (1/2)F_n V$ where $F_n = \dot{M}V$ and $V = F_n/\dot{M}$. With the consistent use of SI units, mechanical power is in watts if net thrust, F_n, is in newtons and effective velocity V is in meters per second. The example in Fig. 5 shows an equivalent mechanical power of 13.13 MW. [The corresponding equivalent mechanical power for the CF6-50C was nearly 38 MW at the takeoff thrust setting.]

Acoustic efficiency was calculated from the ratio of acoustic power to jet-stream mechanical power. Figure 5 shows the flat-weighted and A-weighted efficiencies as 7.8×10^{-5} and 4.6×10^{-5}, respectively. [For the older and noisy JT4A-3 engine, the acoustic efficiency of flat-weighted sound power was significantly greater at 290×10^{-5} for an equivalent mechanical power at takeoff thrust of approximately 22 MW.]

Sound power levels in the forward (0 degrees to 90 degrees) and rear (90 degrees to 180 degrees) quadrants were calculated and are also listed at the foot of the tabulations on Fig. 5.

The noise-evaluation quantity for certification is given, with Eq. (2), by

$$L_{WA} - 10 \lg(F_n c_\infty/\Pi_{ref}) =$$

$$147.8 - 10 \lg(97{,}900 \times 346/1) = 72.5 \text{ dB}$$

for A-weighted sound power level and

$$150.1 - 75.3 = 74.8 \text{ dB}$$

for flat-weighted sound power level.

This Section has described the analysis method and its application to one set of typical test data. The next Section presents the results of the analyses of the data in terms of the recommended noise-evaluation quantity.

RESULTS

Numerical results of the study are given in tabular form in Table 3 and in a graphical format in Figs. 6 and 7.

Table 3 lists the values of the nondimensional sound power [A-frequency weighted and flat or unweighted] and corresponding values of nondimensional thrust for the 15 engines, 41 test configurations, and 190 test conditions. A link between the tabulated data and the configuration of the engine at the time of the test is given by a reference in Table 3 to the corresponding entry in Table 1 or Table 2.

The graphical presentations in Fig. 6, for nondimensional A-weighted sound power, and in Fig. 7, for flat-weighted sound power, illustrate the ability of the recommended noise-evaluation quantity to generalize and correlate the sound produced by a wide range of engine types and test configurations.

For many of the production engines in Fig. 6(a), [remembering that the test configuration was not always representative of an airplane installation],

there was relatively little increase in nondimensional A-weighted sound power with increase in nondimensional thrust or effective jet velocity. Because the A frequency weighting reduces the contribution of low-frequency sounds, such behavior indicates that some source(s) of relatively high-frequency sound (e.g., turbomachinery noise) had nearly constant strength over a range of engine power settings.

Over a wide range of engine power settings, the A-weighted noise-evaluation quantity in Fig. 6(a) had a value between 70 dB and 75 dB, except for the older, noisy JT3D-3B, the JT8D-15 in the untreated, hardwall configuration, and the military TF34-GE-100 at the two highest power settings.

The data in Fig. 6(a)(2) for the military TF34-GE-100 engine and the commercial CF34 show the significant acoustical benefit that resulted from the changes which were made to derive the commercial engine from the military version. Although, as shown by the data in Table 4(a) of Ref. 1, the fan rotor blades of the CF34 are relatively close to the downstream fan-exit stator vanes, the blade-vane spacing for the CF34 was increased slightly over that in the TF34. More importantly, however, the number of fan-exit stator vanes was increased so that propagation of fan noise at the fundamental blade-passage frequency would be cut off at approach power settings. Use of these noise-control design measures in this closely coupled engine yielded the significant reduction of five to six decibels in A-weighted sound power level at thrust settings ranging from approach to takeoff. Larger reductions in the sound pressure level at the fundamental blade-passage frequency are understood to have been achieved.

The experimental YF-102 engine in Fig. 6(b) was tested without sound-absorbing linings in the inlet or exhaust ducts. The test configurations were intended to investigate the effect of different nozzle configurations on jet exhaust noise. The difference between the noisiest and the quietest configurations was approximately three decibels. In terms of the A-weighted noise-evaluation quantity, the noise from the QSRA/YF-102 was comparable to that from many of the more-recent designs for production turbofan engines as well as the experimental JT8D-109 NASA Refan and other low-to-moderate thrust engines in Fig. 6(a)(2).

The experimental Engine A and Engine C from the NASA/GE "Quiet Engine Program" produced normalized A-weighted sound power levels that were generally between 60 dB and 70 dB for a great variety of inlet and exhaust duct configurations, see Figs. 6(c) and 6(d). Those engines, however, were only intended to serve to demonstrate acoustical technology for suppression of turbomachinery noise. The nondimensional A-weighted sound power per unit thrust was able to quantify the differences between the noise from the various test configurations, most of which are shown on Figs. 6(c) and 6(d). Data for all configurations are given in Table 3.

For Engine A [Fig. 6(c)], the difference between the noisiest and the quietest of the test configurations was approximately ten decibels. However, the noisiest test configuration had an inlet duct with simulated blow-in doors. When the blow-in-door inlet was installed, the A-weighted sound power levels were approximately two decibels greater than when the inlet with no blow-in doors was installed.

The data in Fig. 6(c) also indicate that the addition of one acoustically treated splitter ring in the inlet duct reduced the A-weighted sound power level by approximately four decibels. The addition of two more splitter rings (total of three) yielded one to two decibels additional noise reduction.

For Engine C in Fig. 6(d), the test results revealed several interesting trends. In Fig. 6(d)(1), the data showed the regular increase in noise reduction achieved by the addition to the inlet duct of one treated ring splitter, then two, then three, and finally four ring splitters. Figure 6(d)(2) shows, among other things, that adding a layer of perforate backed by thick honeycomb to the inlet wall in front of the fan rotor blades was effective in reducing fan noise over a wide range of engine power settings, not just at the higher power settings where multiple-pure-tone (MPT) sounds are prevalent.

While the comparisons based on A-weighted sound power in Fig. 6 were considered to be appropriate for possible regulatory purposes, the comparisons in Fig. 7 based on flat-weighted (or unweighted) sound power provide a better correlation of the data from the production, and near-production, engines.

At moderate-to-high engine power settings, clustering of the data in Fig. 7(a) was tighter than in Fig. 6(a) because at those power settings the normalized wideband, flat-weighted sound power tends to be controlled by low-frequency jet noise that is de-emphasized by the A-weighting but which should have nearly the same functional dependence on effective jet velocity for many different engines, see Refs. 5 and 6.

For the JT3D-3B and the JT8D-15 engines in Fig. 7(a)(1) and most engines in Fig. 7(a)(2), at low-to-moderate engine power settings, the variation with effective jet velocity of nondimensional flat-weighted sound power per unit of thrust was less rapid than at higher power settings and was similar to the variation of A-weighted sound power per unit of thrust shown in Fig. 6(a) for all engines and the same range of engine power settings. Such a functional dependence does not detract in any way from the utility of the recommended A-weighted noise-evaluation quantity for correlation of the measurements of the total noise from a variety of engines or for its potential use in a requirement for certification of engine noise.

The reason for the similar behavior of the flat-weighted and A-weighted sound power at the low-to-moderate engine thrust settings is likely that the spectrum of the sound for those engines and at those engine conditions consisted mainly of contributions from high-frequency turbomachinery noise such that the two sound power levels were nearly equal. Data in Table 3 provide several examples where the normalized flat-weighted and A-weighted sound power levels are nearly equal at the lower values of normalized thrust (or normalized effective jet velocity).

Turning again to the moderate-to-high-thrust data in Fig. 7(a)(1), inspection of the plotted results indicated that the general trend of the data could be approximated by a fifth-power dependence on normalized jet velocity, at least over a range of normalized effective jet velocity from approximately 0.6 to 1.5. Note, however, that for high-bypass-ratio engines, the greatest measured value of $F_n/\dot{M}c_\infty$ was between 0.9 and 1.0.

In equation form, the approximate fifth-power dependence may be written as

$$10 \lg\left[\frac{W_T/W_{ref}}{F_n c_\infty/\Pi_{ref}}\right] = 50 \lg(F_n/\dot{M}c_\infty) + K \qquad (17)$$

where K is a constant to be determined from the data at $F_n/\dot{M}c_\infty = 1.0$. A slight extrapolation may be required to evaluate K for high-bypass-ratio turbofans.

The fifth-power dependence (or a 50 dB/decade trend slope) also applied rather well to the moderate-to-high-thrust data in Fig. 7(b) for the experimental YF-102 engine and for most data in Fig. 7(c) for Engine A. Some of the data in Fig. 7(c) for Engine A do, however, indicate a trend line with a slope of less than 50 dB/decade.

On the other hand, the data in Fig. 7(d)(1) and 7(d)(2) indicated much shallower slopes ranging from 30 to 33 dB/decade, to as much as 36.5 dB/decade, but never as steep as 50 dB/decade.

Note that, because of the contribution of low-frequency noise, the flat-weighted sound power per unit thrust did not provide the same indication of the noise reduction achieved by acoustical treatment in the inlet and exhaust ducts as did A-weighted sound power per unit thrust. Compare the results of various test configurations for Engines A and C in Figs. 6(c) and 7(c) and 6(d) and 7(d).

Another observation from examination of the flat-weighted and A-weighted sound power data [seen in Fig. 7(a) but perhaps more clearly in Fig. 6(a)] was that a remarkable reduction in sound power per unit thrust has been achieved. There was a difference of the order of ten decibels between the A-weighted sound power per unit thrust produced by the JT3D engine [designed in the late 1950s] and that produced by engines from the early 1970s, such as the CF6-50C and JT9D-70. Comparable reductions in low-frequency jet noise were of the order of 5 decibels, which is still significant considering that the large high-bypass-ratio turbofans produce approximately three times as much static thrust as the smaller low-bypass-ratio turbofans.

It is worthwhile to note that the noise from the two turbojet engines [i.e., the JT4A-3 and the Olympus OL-593 in Fig. 7(a)] was well correlated with the noise produced by the turbofan engines, although the sound power per unit thrust and the effective jet velocity were both much greater. The flat-weighted sound power level from the OL-593 engine was approximately 20 dB greater than that from the CF6-50C or the JT9D-70 engines.

Lastly, we consider the acoustic efficiency as the ratio of sound power to jet-stream mechanical power. The value of the acoustic efficiency may be obtained directly from the data in, for example, Fig. 7 by the ratio of an ordinate value to an abscissa value for a given data point.

To determine the value of acoustic efficiency, first determine the ratio of powers from an ordinate value, i.e., from

$$W_T/F_n c_\infty = 10^{0.1(Y - 120)} \qquad (18)$$

where Y is the ordinate value in decibels as defined by

$$Y = 10 \lg\left[\frac{W_T/W_{ref}}{F_n c_\infty/\Pi_{ref}}\right] \tag{19}$$

and the constant of 120 dB comes from use of the reference acoustic power of 1 pW and the reference mechanical power of 1 W.

The abscissa value is read directly from the $F_n/\dot{M}c_\infty$ scale.

Division of an ordinate value by an abscissa value and introduction of a factor of (1/2) to calculate mechanical jet-stream power as $(1/2)FV$ gives

$$\frac{W_T/F_n c_\infty}{(1/2)[F_n/\dot{M}c_\infty]} = \frac{W_T}{(1/2)F_n V_{eff}} \tag{20}$$

where $V_{eff} = F_n/\dot{M}$.

Two examples from Fig. 7(a) yield an acoustic efficiency of 0.33×10^{-4} for an ordinate/abscissa combination of 70 dB and 0.6, and of 2×10^{-4} for 80 dB and 1.0. Acoustic efficiencies of the order to 10^{-4} have been reported in the literature for jet noise when the Mach number of the jet exhaust is approximately sonic.

The acoustic efficiency of the noisier turbojet engines was much higher. For the OL-593 at maximum thrust without afterburning, the acoustic efficiency was approximately 74×10^{-4} for the combination of 99 dB and $F_n/\dot{M}c_\infty = 2.15$.

CONCLUDING REMARKS

The central purpose of the total study reported in this and companion reports [1,2] was to assess the feasibility of establishing noise-certification standards for future-design turbofan engines. On the basis of the analyses that were performed, it appeared that it is technically feasible to create engine-noise-certification standards. A test procedure can be specified [2] that should yield repeatable and reproducible values for the sound power levels produced by a turbofan engine under acoustical reference conditions.

Noise produced by an engine could be regulated by a quantity which provides a reasonable measure of advances in noise-control technology for both externally-generated jet noise and internally-generated turbomachinery noise. Implementation of a program to reduce engine noise, as measured by changes in the recommended noise-certification quantity, would supplement the continuing requirements in FAR Part 36 for certification of airplane noise.

It was not possible to make a complete assessment of the feasibility of establishing an engine-noise-certification regulation. Engine-installation effects and the effects of flight on the various sources of engine noise were not quantified. No applicable economic data could be obtained to evaluate the economic impact of implementing an engine-noise-certification rule. No assessments were made of the potential changes in community noise levels that might accompany such a regulation.

The principal acoustical measures that were considered as candidates for regulating engine noise were (1) the maximum noise level in the forward or aft quadrants (along a sideline or an arc around an engine reference point), or (2) the sound power level. The A-frequency-weighted sound power level was selected as the basic acoustical parameter in the noise-evaluation quantity.

To make the selected noise-evaluation quantity apply to the wide spectrum of engines that are, or will be, designed for commercial aircraft, the A-weighted sound power was normalized by the total net static thrust produced by the engine as installed on an outdoor test stand and equipped with reference inlet and exhaust ducts [2]. The ratio of the A-weighted sound power, W_A, to the total net thrust, F_n, was then made nondimensional by the reference-day speed of sound, c_∞. The recommended quantity is symbolized by $W_A/F_n c_\infty$. With the decibel as the unit, relative to the standard reference acoustic power, W_{ref}, of one picowatt and a reference mechanical power, Π_{ref}, of one watt, the recommended noise-evaluation quantity is given by

$$10 \lg[(W_A/W_{ref})/(F_n c_\infty/\Pi_{ref})].$$

The merits of the recommended noise-evaluation quantity are: (1) it provides a meaningful and objective measure of the effectiveness of noise-reduction features incorporated into engines, (2) the components of the quantity can be determined from tests such as those often made by the engine manufacturers, (3) the quantity lends itself to a simple, but meaningful, interpretation in a regulatory application.

The proposal developed for an engine-noise-*certification* concept was that particular limits, in decibels, be selected for the value of $10 \lg[(W_A/W_{ref})/(F_n c_\infty/\Pi_{ref})]$. The limiting values should be those considered appropriate for two specified engine power settings.

The selected noise-certification limits would apply to any engine regardless of design, thrust rating, or bypass ratio. Selection of appropriate values for the regulatory limits would be the responsibility of the certifying authority and would require additional study. The recommended engine power settings for demonstration of compliance with the noise-certification standards are: (1) static takeoff-rated thrust, and (2) some fraction of takeoff-rated thrust representative of an in-flight approach power setting.

This report presented results of analyses of farfield sound pressure levels measured around fifteen engines. The engines included eleven production versions and four experimental versions. The analyses included examinations of sound power levels with and without the A-frequency weighting. Results were presented in terms of the nondimensional net total thrust $F_n/\dot{M}c_\infty$ or effective jet Mach number V_{eff}/c_∞ where $V_{eff} = F_n/\dot{M}$ and $\dot{M}$ is the total mass flow rate of air into the engine.

Data from the fifteen engines showed that the recommended noise-evaluation quantity provided a good correlation of the test results and would be a suitable candidate for use in a requirement for certification of engine noise.

A general conclusion from observation of the test data was that future reductions in engine noise will require the design of engines so that the specific thrust (thrust per unit mass flow rate) is as low as practical. Sound-absorbing material and other design features would then be incorporated to further reduce noise from turbomachinery stages.

Table 1. Test configurations for production engines.

item	engine	description
1	JT15D-1	general-aviation P&WA turbofan, NASA-Lewis test run AR 54-1, inflow-control device ICD No. 1, no exhaust-noise muffler, hardwall inlet and exhaust ducts, separate-flow nozzles [Ref. 7]
2	TF34-GE-100	GE turbofan used on A-10A airplane; hardwall production ducts [Ref. 8]
3	CF34	GE turbofan used on Canadair Challenger 601 airplane; commercial derivative of military TF34; production hardwall ducts [Ref. 9]
4	JT4A-3	P&WA turbojet used on initial models of DC-8 and 707 airplanes; round conical nozzle [Ref. 10]
5	JT3D-3B	P&WA turbofan used on DC-8 and 707 airplanes; production hardwall DC-8 short fan duct [Ref. 11]
6	JT8D-15	P&WA turbofan used on DC-9, 727, and 737 airplanes; hardwall bellmouth inlet, hardwall fan duct and tailpipe [Ref. 12]
7	JT8D-209	P&WA turbofan used on MD-80 airplanes; hardwall bellmouth inlet, treated fan duct, hardwall tailpipe, 12-lobe internal mixer [Ref. 12]
8	JT9D-70/CNS	P&WA turbofan used on DC-10 and 747 airplanes; treated inlet, treated fan case, treated fan duct, treated tailpipe [Ref. 12]
9	CF6-6D	GE turbofan used on DC-10 airplanes; treated inlet, treated fan case, treated fan duct, treated tailpipe [Ref. 13]
10	CF6-50C	GE turbofan used on DC-10, 747, and A300B airplanes; treated inlet, treated fan case, treated fan duct, treated tailpipe [Ref. 13]
11	OL-593	Rolls Royce (Bristol) Olympus 593 afterburning turbojet engine for Concorde airplanes; production configuration with variable-area nozzle [Ref. 14]

Table 2. Test configurations for experimental engines.

(a) NASA/GE Quiet Engine Program, Engine A [Ref. 15][a].

item	test number	shape	inlet		fan exhaust		turbine exhaust	size of separate-flow nozzles
			treated ring splitters	acoustical treatment on cowl wall	treated ring splitters	acoustical treatment on walls	acoustical treatment on walls	
1	7	bellmouth	none	hardwall	none	hardwall	hardwall	nominal
2	8	"	"	"	"	"	"	small fan nozzle
3	9	"	"	"	"	"	"	large fan nozzle
4	12	"	"	51-cm of MDOF	"	94-cm of MDOF	Cerafelt	nominal
5	14	"	"	hardwall	"	hardwall	MDOF	nominal
6	20-21	simulated blow-in doors	"	"	"	"	"	large fan nozzle
7	25A	bellmouth	3	51-cm of MDOF + 147-cm of SDOF	1	94-cm of MDOF	"	nominal
8	27[b]	"	3	"	1	"	"	"
9	30	"	3	"	1	"	hardwall	"
10	32	"	none	"	1	"	MDOF	"

[a]All test configurations had multiple-degree-of-freedom (MDOF) treatment in fan frame. Single-degree-of-freedom (SDOF) linings where noted.

[b]For this test, engine case was wrapped with sound-absorbing foam and leaded-vinyl.

Table 2. Continued.

(b) NASA/GE Quiet Engine Program, Engine C [Ref. 16][a]

item	configuration	inlet			fan exhaust		turbine exh.	fan nozzle
		shape	treated ring splitters	acoustical treatment on cowl wall	treated splitters	acoustical treatment on walls	acoustical treatment on walls	relative to core nozzle
1	fan frame treated	standard bellmouth	none	38.6-cm of MDOF	none	50.2-cm of MDOF	94-cm of SDOF	upstream
2	fully suppressed[b]	long, contoured bellmouth	4	A + B + C	1	227-cm of Scottfelt	"	upstream
3	suppressed inlet, hardwall fan duct	"	4	A + B + C	none	hardwall	"	upstream
4	coplanar nozzles	"	4	A + B + C	1	227-cm of Scottfelt	"	coplanar
5	fan-noise suppressed hardwall core	"	4	A + B + C	1	"	hardwall	upstream
6	four splitters	long bellmouth + spoolpiece	4	A + D	1	"	94-cm SDOF	"
7	three splitters	"	3	A + D	1	"	"	"
8	two splitters	"	2	A + D	1	"	"	"
9	one splitter	"	1	A + D	1	"	"	"
10	no splitters, long inlet	"	none	A + D	1	"	"	"
11	no splitters, contoured inlet	contoured bellmouth	none	A	1	"	"	"
12	61-cm MPT, long inlet	long, contoured bellmouth	none	A + B	1	"	"	"
13	91-cm MPT, long inlet	"	none	A + B + C	1	"	"	"

[a] All test configurations had MDOF treatment in fan frame and nominal exit areas for exhaust nozzles.
[b] For this test, engine case was wrapped with sound-absorbing foam and leaded-vinyl.
A = 94.7 cm of different thicknesses of SDOF. B = 61 cm of thick SDOF.
C = 30.5 cm of thick SDOF. D = 61 cm of hardwall spool piece.

Table 2. Concluded.

(c) NASA/P&WA JT8D-109 NASA Refan [Ref. 17].

item	run no.	test no.	inlet	fan exhaust	turbine exhaust
1	2295	8	hardwall	hardwall	hardwall
2	2268	2	treated	treated	hardwall
3	2282	4	treated	treated	treated

(d) NASA Quiet STOL Research Aircraft [QSRA], Lycoming YF-102 [Ref. 18][a].

item	test no.	nozzle system
1	AR-C4	confluent exhaust flow, short core nozzle
2	AR-C5	confluent exhaust flow, large exit nozzle
3	AR-C6	confluent exhaust flow, small core nozzle
4	AR-S3	separate exhaust flows, small core nozzle

[a]All test configurations had a hardwall bellmouth inlet and hardwall fan-discharge and turbine-discharge ducts.

Table 3. Engine noise levels in terms of recommended noise-evaluation quantity.

(a) Production engines.

item	engine	Table reference[a]	$F_n/\dot{M}c_\infty$	$10 \lg \left[\frac{W_T/W_{ref}}{F_n c_\infty/\Pi_{ref}}\right]$	$10 \lg \left[\frac{W_T/W_{ref}}{F_n c_\infty/\Pi_{ref}}\right]$
1	JT15D-1	1-1	0.301	70.2	71.9
			0.386	69.7	72.0
			0.446	69.1	71.0
			0.497	69.3	71.1
			0.551	69.5	71.6
			0.689	75.8	76.9
			0.794	75.4	77.7
2	TF34-GE-100	1-2	0.199	65.9	67.1
			0.277	67.5	68.1
			0.487	74.6	74.4
			0.618	77.4	77.7
			0.791	81.5	82.3
3	CF34	1-3	0.41	66.1	66.8
			0.44	67.3	67.7
			0.45	67.5	68.4
			0.47	69.6	70.8
			0.53	69.9	71.1
			0.57	72.6	73.8
			0.59	75.5	76.9
			0.77	74.3	76.0
			0.80	74.8	77.0
			0.82	76.1	78.1
4	JT4A-3	1-4	1.77	89.0	94.1
5	JT3D-3B	1-5	0.287	70.4	70.0
			0.626	78.1	78.0
			0.681	78.3	78.5
			0.746	78.1	79.0
			0.845	79.4	81.4
			0.945	81.3	83.9
			1.003	80.9	85.5
			1.088	80.8	87.5

[a]See Table 1 for descriptions of test configurations.

Table 3. Continued.

(a) Production engines (Concluded).

Item	Engine	Table reference	$F_n/\dot{m}c_\infty$	$10 \lg\left[\frac{W_T/W_{ref}}{F_n c_\infty/\Pi_{ref}}\right]$	$10 \lg\left[\frac{W_T/W_{ref}}{F_n c_\infty/\Pi_{ref}}\right]$
6	JT8D-15	1-6	0.624	76.9	77.1
			0.727	77.5	78.0
			0.917	77.3	79.3
			1.103	78.6	82.7
			1.265	80.7	85.8
			1.453	83.8	88.9
7	JT8D-209	1-7	0.620	69.7	71.1
			0.715	70.1	72.5
			0.817	73.4	75.3
			0.946	73.2	76.9
			0.993	73.8	77.9
			1.133	76.5	81.6
8	JT9D-70/CNS	1-8	0.555	66.8	67.7
			0.592	68.0	69.0
			0.756	69.7	73.2
			0.802	69.7	74.4
			0.855	69.9	75.5
			0.887	70.3	77.2
9	CF6-6D	1-9	0.526	68.5	69.1
			0.599	70.0	70.8
			0.782	72.4	74.5
			0.842	72.3	75.1
10	CF6-50C	1-10	0.581	69.0	69.9
			0.630	70.6	71.5
			0.905	71.6	76.0
			0.985	72.5	78.2
11	OL-593	1-11	2.15	—	98.9
			2.45	—	99.9

Table 3. Continued.

(b) Experimental engines.

item	engine	Table reference[b]	$F_n/\dot{M}c_\infty$	$10 \lg\left[\frac{W_A/W_{ref}}{F_n c_\infty/\Pi_{ref}}\right]$	$10 \lg\left[\frac{W_T/W_{ref}}{F_n c_\infty/\Pi_{ref}}\right]$
1	QEP-A	2(a)-1	0.476	65.2	66.1
			0.728	71.0	74.0
2	QEP-A	2(a)-2	0.552	67.7	68.9
			0.646	69.5	71.1
3	QEP-A	2(a)-3	0.554	65.5	66.9
4	QEP-A	2(a)-4	0.476	63.4	64.9
			0.548	64.9	67.2
			0.630	67.5	70.3
			0.728	68.5	72.9
5	QEP-A	2(a)-5	0.476	65.0	65.9
			0.548	67.1	68.5
			0.728	71.5	73.9
6	QEP-A	2(a)-6	0.462	67.0	67.3
			0.554	69.7	70.0
			0.630	71.3	71.9
			0.712	72.5	74.3
7	QEP-A	2(a)-7	0.476	57.9	61.7
			0.548	60.1	64.7
			0.630	61.9	67.5
			0.728	64.5	71.7
8	QEP-A	2(a)-8	0.476	59.0	62.5
			0.548	60.4	64.9
			0.630	62.1	68.1
			0.728	64.5	71.6
9	QEP-A	2(a)-9	0.476	57.5	61.8
			0.548	59.7	65.1
			0.630	61.4	67.7
			0.728	64.2	71.6
10	QEP-A	2(a)-10	0.476	60.0	63.0
			0.548	61.8	65.8
			0.630	63.5	68.5

[b]See Table 2 for descriptions of test configurations.

Table 3. Continued.

(b) Experimental engines (Continued).

item	engine	Table reference	$F_n/\dot{m}c_\infty$	$10 \lg \left[\frac{W_A/W_{ref}}{F_n c_\infty/\Pi_{ref}}\right]$	$10 \lg \left[\frac{W_T/W_{ref}}{F_n c_\infty/\Pi_{ref}}\right]$
11	QEP-C	2(b)-1	0.458	68.1	68.7
			0.557	71.6	71.8
			0.657	77.5	77.4
			0.775	77.5	78.8
12	QEP-C	2(b)-2	0.458	60.3	62.6
			0.557	61.8	65.3
			0.657	62.8	66.5
			0.775	64.6	69.3
13	QEP-C	2(b)-3	0.458	65.2	66.9
			0.557	68.2	69.6
			0.657	70.0	71.5
			0.775	72.2	74.0
14	QEP-C	2(b)-4	0.458	60.7	62.7
			0.557	61.7	64.7
			0.657	63.2	67.0
			0.775	65.7	70.6
15	QEP-C	2(b)-5	0.458	62.7	64.2
			0.557	63.6	66.4
			0.657	64.4	67.4
			0.775	67.2	70.8
16	QEP-C	2(b)-6	0.458	60.3	62.7
			0.557	61.6	65.0
			0.657	63.9	67.4
			0.775	66.5	71.4
17	QEP-C	2(b)-7	0.458	62.5	64.7
			0.557	63.2	66.2
			0.657	64.9	67.9
			0.775	67.3	71.5
18	QEP-C	2(b)-8	0.458	63.3	64.9
			0.557	64.6	67.0
			0.657	67.4	69.4
			0.775	67.7	71.5

Table 3. Continued.

(b) Experimental engines (Continued).

item	engine	Table reference	$F_n/\dot{m}_{C_\infty}$	$10 \lg\left[\frac{\dot{m}_A/\dot{m}_{ref}}{F_n C_\infty/\Pi_{ref}}\right]$	$10 \lg\left[\frac{\dot{m}_T/\dot{m}_{ref}}{F_n C_\infty/\Pi_{ref}}\right]$
19	QEP-C	2(b)-9	0.458	63.2	64.8
			0.557	66.2	68.0
			0.657	68.2	69.6
			0.775	68.8	72.0
20	QEP-C	2(b)-10	0.458	64.1	65.1
			0.557	67.5	68.4
			0.657	70.2	70.8
			0.775	71.7	74.2
21	QEP-C	2(b)-11	0.458	65.4	66.3
			0.557	69.0	69.5
			0.657	71.8	72.4
			0.775	72.5	74.8
22	QEP-C	2(b)-12	0.458	63.6	65.0
			0.557	66.4	67.8
			0.657	68.5	69.5
			0.775	69.5	72.0
23	QEP-C	2(b)-13	0.458	63.1	64.5
			0.557	64.5	66.4
			0.657	66.9	68.7
			0.775	68.3	71.5
24	JT8D-109	2(c)-1	0.610	72.5	73.2
			0.610	72.8	73.5
			0.610	73.1	73.7
			0.829	74.6	76.2
			0.829	75.5	77.3
			0.829	74.9	76.5
			1.000	76.3	80.0
			1.000	76.6	80.3
25	JT8D-109	2(c)-2	0.610	69.3	71.0
			0.610	69.5	71.1
			0.610	69.8	71.4
			0.615	69.7	71.3
			0.829	72.3	75.3
			0.829	72.4	75.4
			0.829	72.4	75.4
			0.829	72.6	75.6
			0.966	75.7	79.7
			0.969	75.8	79.7
			0.969	76.0	80.2

Table 3. Concluded.

(b) Experimental engines (Concluded).

Item	Engine	Table reference	$F_n/\delta c_\infty$	$10 \lg \left[\frac{W_A/W_{ref}}{F_n c_\infty/\pi_{ref}}\right]$	$10 \lg \left[\frac{W_T/W_{ref}}{F_n c_\infty/\pi_{ref}}\right]$
26	JT8D-109	2(c)-3	0.610	68.9	70.9
			0.610	69.0	70.9
			0.610	68.9	70.8
			0.822	71.4	75.1
			0.822	71.2	74.8
			0.836	71.1	74.9
			1.006	75.4	80.2
			1.008	75.2	79.4
27	QSRA/YF-102	2(d)-1	0.393	66.1	67.1
			0.473	67.3	68.7
			0.607	70.8	72.2
			0.717	74.8	76.2
			0.841	74.8	78.9
28	QSRA/YF-102	2(d)-2	0.356	68.1	68.8
			0.434	69.3	70.1
			0.556	71.3	72.0
			0.639	75.5	75.8
			0.749	76.3	77.8
29	QSRA/YF-102	2(d)-3	0.385	64.8	65.6
			0.467	66.7	67.6
			0.604	68.5	70.5
			0.618	68.9	70.6
			0.710	71.9	74.5
			0.797	74.9	78.1
30	QSRA/YF-102	2(d)-4	0.377	66.3	67.2
			0.456	68.1	69.0
			0.585	69.8	70.8
			0.690	73.9	75.0
			0.792	76.0	78.4

VOLUME III NASA / GE Q U I E T E N G I N E C PAGE 31

CONFIGURATION - C O N T O U R E D I N L E T - NOMINAL NOZZLE
CONTOUR INLET / NO SPLITTERS 94.7 CM SDOF INLET THT
MDOF FAN FRAME, COMP. INLET / SCOTTFELT FAN EXH / SDOF CORE EXH

SOURCE - NASA QUIET ENGINE PROGRAM /GE/ NASA CR-121176 NAS3-12430
TEST SITE - PEEBLES,OHIO - 46.5 M ARC - 12.2 M POLE MICROPHONES
DESIGN POINT - THRUST-97.9 KN ; N1-4948 RPM ; BPR-5.0 ; 415 KG/S

TEST DATE : 04-11-72
RUN NUMBR : QEPC-90
THRUST = 97.9 KN

M TOT = 365.1 KG/S
EFF VJ = 268.1 M/S

ENGINE HT = 4.0 M
EFF DIAM = 1.4 M
ENG BPR = 5.0

GND SURFC : GRAVEL
SIGMA = 0.0 RYL/CM
MIC HT = 12.2 M

DISTANCE = 46.5 M RADIUS
AMB TEMP = 15.0 DEG C
REL HUMID = 70.0 PCT

INPUT SOUND PRESSURE LEVELS, DB

	BND NUM	CMF ,HZ	STRHL NUMBR	ANGLE FROM INLET CENTERLINE, DEGREES 10.0	20.0	30.0	40.0	50.0	60.0	70.0	80.0	90.0	100.0	110.0	120.0	130.0	140.0	150.0
1	17	50	0.261	83.5	82.0	81.7	82.7	85.8	82.5	83.7	85.8	86.8	86.7	89.6	90.9	92.8	95.0	101.7
2	18	63	0.329	83.7	82.0	80.7	81.2	86.7	82.8	83.6	85.2	87.0	86.7	89.7	91.4	92.2	93.9	98.0
3	19	80	0.418	84.5	83.8	84.3	82.6	87.3	84.6	83.2	84.6	85.5	85.5	88.6	90.9	91.9	93.6	96.6
4	20	100	0.522	84.6	83.1	83.6	83.1	87.9	82.9	84.8	86.8	87.8	89.7	91.6	93.3	94.9	97.1	100.0
5	21	125	0.653	85.1	85.2	86.9	86.1	91.0	88.3	90.2	91.5	92.3	93.3	94.9	96.6	96.2	99.5	102.4
6	22	160	0.835	86.9	88.1	91.9	92.0	93.0	92.0	93.6	92.2	94.0	93.7	96.7	97.1	99.0	99.0	100.8
C	23	200	1.044	86.6	87.9	88.9	90.3	92.1	90.1	88.7	90.3	92.3	93.0	95.0	95.1	95.9	97.1	97.0
E	24	250	1.305	90.1	87.3	86.6	86.2	90.1	88.8	90.7	90.1	91.1	91.1	93.0	93.2	94.9	95.2	95.0
N	25	315	1.645	88.8	92.5	90.8	91.3	94.9	93.8	96.7	99.1	97.3	93.1	94.0	95.1	94.0	94.8	95.0
T	26	400	2.088	91.9	92.2	97.6	98.9	100.9	104.7	103.5	100.8	95.9	96.7	100.5	97.2	93.9	97.9	96.9
E	27	500	2.611	97.8	96.5	98.6	99.4	103.6	100.7	103.2	101.8	102.8	100.9	100.2	94.3	95.8	95.0	98.7
R	28	630	3.289	96.0	97.3	100.0	98.5	99.1	98.1	99.1	96.5	96.5	91.1	95.2	92.6	93.4	94.1	95.0
F	29	800	4.177	97.0	96.4	96.8	93.0	95.0	97.1	95.8	93.1	96.1	93.3	94.1	94.5	94.1	92.9	92.0
R	30	1000	5.221	98.1	101.3	97.0	97.5	98.3	96.0	94.9	96.3	95.5	92.1	93.9	94.6	91.2	92.2	93.2
E	31	1250	6.526	89.0	98.1	97.8	96.3	96.1	98.8	93.7	93.3	94.1	90.1	91.0	91.4	89.0	92.2	91.8
Q	32	1600	8.358	97.9	96.2	97.9	94.4	94.0	97.0	93.0	92.2	92.1	89.0	89.1	89.4	89.1	90.2	89.9
U	33	2000	10.442	101.9	101.3	100.2	98.2	96.9	95.2	93.8	94.2	90.3	89.0	90.9	88.5	90.1	89.4	90.1
E	34	2500	13.053	100.6	99.3	99.5	98.9	95.8	92.5	93.9	93.2	91.2	90.0	90.6	88.0	88.8	89.1	89.9
N	35	3150	16.446	96.2	97.3	98.1	95.2	94.3	90.3	91.1	90.2	90.3	87.1	87.9	89.4	86.4	87.1	87.2
C	36	4000	20.884	98.7	96.0	96.4	96.9	93.7	92.6	90.4	91.9	88.0	87.6	88.6	88.1	88.8	87.6	87.8
Y	37	5000	26.105	96.1	97.5	94.9	94.4	93.2	90.0	90.9	90.4	88.1	84.1	86.9	86.1	85.3	87.3	85.1
H	38	6300	32.893	95.2	94.3	95.2	95.5	92.0	88.2	88.9	89.1	87.3	85.8	86.9	86.2	86.2	85.7	86.8
E	39	8000	41.766	92.0	94.1	92.7	93.9	89.6	88.0	87.8	87.1	87.1	83.9	85.6	85.3	85.2	84.9	82.9
R	40	10000	52.210	89.7	90.1	89.9	91.8	89.5	83.7	85.3	83.9	84.9	82.7	87.7	88.7	86.7	84.9	83.7
Z																		
	OASPL: DB			109.2	109.6	109.6	108.9	109.5	109.4	109.3	108.2	107.8	106.0	107.6	106.7	107.1	108.1	110.0
	AL : DB			109.3	109.8	109.4	108.3	107.8	107.5	106.9	105.6	105.3	102.9	104.2	102.8	102.2	102.6	103.3
	PNL : DB			122.3	122.1	122.4	121.6	120.3	119.2	118.7	118.3	117.7	115.8	116.9	116.3	116.1	116.4	117.1
	PNLT : DB			123.5	123.3	122.4	121.6	120.3	119.2	118.7	118.3	117.7	115.8	116.9	116.3	116.1	116.4	117.1
	TCORR: DB			1.2	1.2	0.0	0.0	0.0	0.0	0.0	0.0	0.0	0.0	0.0	0.0	0.0	0.0	0.0
	TCBND			33	33	17	17	17	17	17	17	17	17	17	17	17	17	17

Fig. 1. Sample page of input sound pressure level data.

CONFIGURATION = C O N T O U R E D I N L E T = NOMINAL NOZZLE
CONTOUR INLET / NO SPLITTERS 94.7 CM SDOF INLET TMT
NDOF FAN FRAME, COMP. INLET / SCOTTFELT FAN EXH / SDOF CORE EXH

SOURCE = NASA QUIET ENGINE PROGRAM /GE/ NASA CR-121176 NAS3-12438
TEST SITE = PEEBLES,OHIO - 46.5 M ARC = 12.2 M POLE MICROPHONES
DESIGN POINT = THRUST=97.9 KN ; N1=4940 RPM ; BPR=5.0 ; 415 KB/S

TEST DATE = 04-11/72 M TOT = 305.1 KG/S ENGINE HT = 4.0 M GND SURFC = GRAVEL DISTANCE = 61.0 M SIDLNE
RUN NUMBR = QEPC-98 EFF VJ = 268.1 M/S EFF DIAM = 1.4 M SIGMA = 0.0 RYL/CM AMB TEMP = 25.0 DEG C
THRUST = 97.9 KN ENG BPR = 5.0 MIC HT = 12.2 M REL HUMID = 70.0 PCT

61.0 M S I D E L I N E S P L S , D B

	BND NUM	GMF MHZ	STRHL NUMBR	A N G L E F R O M I N L E T C E N T E R L I N E , D E G R E E S 10.0	20.0	30.0	40.0	50.0	60.0	70.0	80.0	90.0	100.0	110.0	120.0	130.0	140.0	150.0
1	17	50	0.261	65.8	70.3	73.3	76.5	81.1	78.9	80.8	83.3	84.4	84.2	86.7	87.3	88.1	88.8	93.3
2	18	63	0.329	66.0	70.3	72.3	75.0	82.0	79.2	80.7	82.7	84.6	84.2	86.4	87.8	87.5	87.7	89.6
3	19	80	0.418	66.8	72.1	75.9	76.4	82.6	81.0	80.3	82.1	83.1	83.8	85.7	87.3	87.2	87.4	88.2
0	20	100	0.522	66.9	71.3	75.2	76.9	83.2	79.3	81.9	84.3	85.4	87.2	88.7	89.7	90.2	90.9	91.6
8	21	125	0.653	67.3	73.4	78.5	79.9	86.3	84.7	87.3	89.8	89.9	90.8	92.0	93.0	93.5	93.3	93.6
8	22	160	0.835	69.0	76.3	83.4	85.8	88.3	88.4	90.7	89.7	91.6	91.2	93.8	93.5	94.3	92.8	92.3
•	23	200	1.044	68.7	76.1	80.4	84.0	87.4	86.5	85.8	87.8	89.9	90.5	92.1	91.5	91.2	90.8	88.5
C	24	250	1.305	72.1	78.4	78.1	79.9	85.4	85.1	87.8	87.6	88.7	88.6	90.1	89.5	90.2	88.9	86.5
E	25	315	1.645	70.7	80.6	82.3	85.0	90.2	90.1	93.8	96.6	94.9	90.6	91.1	91.4	89.3	88.6	86.5
N	26	400	2.088	73.6	80.2	89.0	92.6	96.1	101.0	100.5	98.3	93.5	94.2	97.5	93.5	89.1	91.6	88.3
T	27	500	2.611	70.3	87.1	90.9	93.5	98.8	97.0	100.5	98.2	100.4	98.2	97.5	90.5	87.0	84.6	90.1
E	28	630	3.289	77.3	85.1	91.3	92.1	94.3	94.4	96.1	93.9	94.1	88.5	92.2	88.9	88.6	87.7	86.3
F	29	800	4.177	78.0	84.1	88.0	86.5	90.1	93.3	92.8	90.5	93.6	90.7	91.1	90.7	89.2	86.4	83.2
R	30	1000	5.221	78.7	88.8	88.1	91.0	93.4	92.2	91.8	93.7	93.0	89.5	90.8	90.8	86.3	85.7	84.3
E	31	1250	6.526	69.1	85.4	88.8	89.7	91.1	95.0	90.6	90.6	91.6	87.4	87.9	87.6	84.0	85.6	82.8
Q	32	1600	8.354	77.4	83.2	88.7	87.7	88.9	93.1	89.9	89.5	89.5	86.3	86.0	85.5	84.0	83.5	80.7
U	33	2000	10.442	80.6	88.8	90.8	91.3	90.8	91.2	90.6	91.4	87.7	86.2	87.7	84.5	85.1	82.5	80.7
E	34	2500	13.053	78.3	85.5	94.3	91.9	90.5	88.4	90.6	90.4	88.5	87.2	87.3	83.9	83.6	82.1	80.3
N	35	3150	16.446	72.7	83.0	88.2	88.0	88.9	86.2	87.8	87.3	87.6	84.2	84.6	85.3	81.0	79.9	77.3
C	36	4000	20.884	73.5	81.0	86.6	89.5	88.2	88.4	87.3	89.0	85.3	84.7	85.2	83.9	83.3	80.4	77.6
Y	37	5000	26.105	69.9	82.1	84.4	86.9	87.6	85.6	87.5	87.5	85.4	81.2	83.5	81.9	79.7	79.8	74.6
H	38	6300	32.893	66.8	78.1	84.3	87.8	86.4	84.0	85.6	86.3	84.7	83.8	83.6	82.0	80.6	78.0	75.9
E	39	8000	41.768	60.1	76.6	81.2	85.9	83.9	83.8	84.6	84.4	84.6	81.2	82.4	81.1	79.5	76.9	71.4
A	40	10000	52.210	52.6	70.5	77.5	83.4	83.6	79.5	82.2	81.4	82.6	80.2	84.6	84.5	80.8	76.5	71.3
Z																		
		OASPL, DB		88.3	96.4	100.3	102.1	104.6	105.6	106.3	105.6	105.3	103.4	104.6	103.0	102.3	101.7	101.5
		AL , DB		87.8	96.2	99.9	101.2	102.8	103.7	103.8	103.2	102.8	100.3	101.1	98.9	97.2	96.1	94.3
		PNL , DB		100.2	108.5	112.8	114.6	115.2	115.4	114.6	115.5	115.2	113.1	113.8	112.4	110.6	109.6	107.8
		PNLT , DB		101.4	109.7	112.8	114.6	115.2	115.4	115.6	115.5	115.2	113.1	113.8	112.4	110.9	109.5	107.8
		TCORR, DB		1.2	1.2	0.0	0.0	0.0	0.0	0.0	0.0	0.0	0.0	0.0	0.0	0.0	0.0	0.0
		TCBND		33	33	17	17	17	17	17	17	17	17	17	17	17	17	17

Fig. 2. Sample page with input sound pressure levels adjusted to 61-m sideline and reference atmospheric conditions of 25° C and 70-percent relative humidity.

CONFIGURATION = C O N T O U R E D I N L E T = NOMINAL NOZZLE
CONTOUR INLET / NO SPLITTERS 94.7 CM SDOF INLET TMT
MDOF FAN FRAME, COMP. INLET / SCOTTFELT FAN EXH / SDOF CORE EXH

SOURCE = NASA QUIET ENGINE PROGRAM /GE/ NASA CR-121176 NAS3-12430
TEST SITE = PEEBLES,OHIO - 46.5 M ARC = 12.2 M POLE MICROPHONES
DESIGN POINT = THRUST=97.9 KN ; N1=4940 RPM ; BPR=5.0 ; 415 KG/S

TEST DATE = 04-11/72
RUN NUMBR = QEPC-90
THRUST = 97.9 KN

M TOT = 365.1 KG/S
EFF VJ = 208.1 M/S

ENGINE HT = 4.0 M
EFF DIAM = 1.4 M
ENG BPR = 5.0

GND SURFC = GRAVEL
SIGMA = 0.0 RYL/CM
MIC HT = 12.2 M

DISTANCE = 45.7 M RADIUS
AMB TEMP = 25.0 DEG C
REL HUMID = 70.0 PCT

45.7 M P O L A R R A D I U S S P L S , D B

	BND NUM	CMF ,HZ	STRHL NUMBR	ANGLE FROM INLET CENTERLINE, DEGREES 10.0	20.0	30.0	40.0	50.0	60.0	70.0	80.0	90.0	100.0	110.0	120.0	130.0	140.0	150.0
1	17	50	0.261	83.6	82.1	81.8	82.8	85.9	82.6	83.8	85.9	86.9	86.6	89.7	91.0	92.9	95.1	101.8
2	18	63	0.329	83.8	82.1	80.8	81.3	86.8	82.3	83.7	85.3	87.1	86.8	89.8	91.5	92.3	94.0	98.1
3	19	80	0.418	84.6	83.9	84.4	82.7	87.4	84.7	83.3	84.7	85.6	85.6	88.7	91.0	92.0	93.7	96.7
0	20	100	0.522	84.7	83.2	83.7	83.2	88.0	83.0	84.9	86.9	87.9	89.8	91.7	93.4	95.0	97.2	100.1
.	21	125	0.653	85.2	85.3	87.0	86.2	91.1	88.4	90.3	91.6	92.4	93.4	95.0	96.7	98.3	99.6	102.1
B	22	160	0.835	87.0	88.2	92.0	92.1	93.1	92.1	93.7	92.3	94.1	93.8	96.8	97.2	99.1	99.1	100.9
.	23	200	1.044	86.7	88.0	89.0	90.4	92.2	90.2	88.8	90.4	92.4	93.1	95.1	95.2	96.0	97.2	97.1
C	24	250	1.305	90.2	87.4	86.7	86.3	90.2	88.9	90.8	90.2	91.2	91.2	93.1	93.3	95.0	95.3	95.1
E	25	315	1.645	88.9	92.6	90.9	91.4	95.0	93.9	96.8	98.2	97.4	93.2	94.1	95.2	94.1	95.0	95.1
N	26	400	2.088	92.0	92.3	97.7	99.0	101.0	104.8	103.6	100.9	96.0	96.8	100.6	97.3	94.0	98.0	97.0
T	27	500	2.611	97.9	98.3	98.7	100.0	103.7	100.8	103.6	101.9	102.9	101.0	100.6	94.3	95.9	95.1	98.8
E	28	630	3.284	96.1	97.4	100.1	98.6	99.2	98.2	99.2	96.6	96.6	91.2	95.3	92.7	93.5	94.2	95.1
F	29	800	4.177	97.1	96.5	96.9	93.1	95.1	97.2	95.9	93.2	96.2	93.4	94.2	94.6	94.2	93.0	92.1
R	30	1000	5.221	98.2	101.4	97.1	97.6	98.4	96.1	95.0	96.4	95.6	92.2	94.0	94.7	91.5	92.3	93.4
E	31	1250	6.526	89.1	98.2	97.9	96.4	96.2	98.9	93.8	93.4	94.2	90.2	91.1	91.5	89.1	92.3	91.9
Q	32	1600	8.354	98.0	96.3	98.0	94.5	94.1	97.1	93.1	92.3	92.2	89.1	89.2	89.5	89.2	90.3	90.0
U	33	2000	10.442	102.0	101.4	100.3	98.3	96.1	95.3	93.9	94.3	90.4	89.1	91.0	88.6	90.4	89.5	90.2
E	34	2500	13.053	100.7	99.4	100.0	99.0	95.9	92.6	94.0	93.3	91.3	90.1	90.7	88.1	89.0	89.2	90.0
N	35	3150	16.446	96.3	97.4	98.2	95.3	94.4	90.4	91.2	90.3	90.4	87.2	88.0	89.5	86.5	87.2	87.3
C	36	4000	20.884	98.9	96.2	97.1	97.1	93.9	92.6	90.9	92.1	88.2	87.8	88.8	88.3	89.0	88.0	86.0
Y	37	5000	26.105	96.3	97.7	95.1	94.6	93.4	90.2	91.1	90.6	88.3	84.3	87.1	86.3	86.5	87.5	85.3
.	38	6300	32.893	95.6	94.7	95.6	95.9	92.4	88.6	89.3	89.5	87.7	86.2	87.3	86.6	86.6	86.1	87.2
M	39	8000	41.768	92.8	94.9	93.5	94.7	90.4	88.8	88.6	87.9	87.9	84.7	86.4	86.1	86.0	85.7	83.7
E	40	10000	52.210	90.9	91.3	91.1	93.0	90.7	84.9	86.5	85.1	86.1	83.9	88.9	89.9	87.9	86.1	84.9
T																		
Z																		
	OASPL; DB			109.3	109.8	109.7	109.1	109.6	109.5	109.4	108.4	107.9	106.1	107.8	106.8	107.2	108.2	110.2
	AL ; DB			109.5	109.7	109.5	108.4	108.5	107.6	107.0	106.0	105.5	103.1	104.3	103.0	102.4	102.9	103.5
	PNL ; DB			122.5	122.3	122.5	121.7	120.5	119.4	118.9	118.4	117.9	115.9	117.0	116.5	116.3	116.5	117.2
	PNLT ; DB			123.6	123.4	122.5	121.7	120.5	119.4	118.9	118.4	117.9	115.9	117.0	116.5	116.3	116.5	117.2
	TCORR; DB			1.2	1.2	0.0	0.0	0.0	0.0	0.0	0.0	0.0	0.0	0.0	0.0	0.0	0.0	0.0
	TCBND			33	33	17	17	17	17	17	17	17	17	17	17	17	17	17

Fig. 3. Sample page with input sound pressure levels adjusted to 45.7-m-radius polar arc and reference atmospheric conditions of 25° C and 70-percent relative humidity.

VOLUME III NASA / GE Q U I E T E N G I N E C PAGE 37

CONFIGURATION - C O N T O U R E D I N L E T - NOMINAL NOZZLE
CONTOUR INLET / NO SPLITTERS 94.7 CM SDOF INLET TMT
MDOF FAN FRAME, COMP. INLET / SCOTTFELT FAN EXH / SDOF CORE EXH

SOURCE - NASA QUIET ENGINE PROGRAM /GE/ NASA CR-121176 NAS3-12430
TEST SITE - PEEBLES,OHIO - 45.5 M ARC - 12.2 M POLE MICROPHONES
DESIGN POINT - THRUST=97.9 KN ; N1=4948 RPM ; BPR=5.0 ; 415 KG/S

TEST DATE = 04-11/72 M TOT = 365.1 KG/S ENGINE HT = 4.0 M GND SURFC = GRAVEL DISTANCE = 45.7 M RADIUS
RUN NUMBR = QEPC-98 EFF VJ = 268.1 M/S EFF DIAM = 1.4 M SIGMA = 0.6 MYL/CM AMB TEMP = 25.0 DEG C
THRUST = 97.9 KN ENG BPR = 5.0 MIC HT = 12.2 M REL HUMID = 70.0 PCT

E N G I N E N O I S E D I R E C T I V I T Y (S P L - S P A V G S P L) , D B

	BND NUM	GMF ,HZ	STRHL NUMBR	ANGLE FROM INLET CENTERLINE, DEGREES 10.0	20.0	30.0	40.0	50.0	60.0	70.0	80.0	90.0	100.0	110.0	120.0	130.0	140.0	150.0
1	17	50	0.261	-10.2	-11.7	-12.0	-11.0	-7.9	-11.2	-10.0	-7.9	-6.9	-7.0	-4.1	-2.8	-.9	1.3	8.0
2	18	63	0.329	-7.6	-8.3	-10.6	-10.1	-4.6	-8.5	-7.7	-6.1	-4.3	-4.6	-1.6	.1	.9	2.9	6.7
3	19	80	0.418	-5.4	-6.1	-5.6	-7.3	-2.6	-5.3	-6.7	-5.3	-4.4	-4.4	-1.3	1.0	2.0	3.7	6.7
0	20	100	0.522	-7.8	-9.3	-8.8	-9.3	-4.5	-9.5	-7.6	-5.6	-4.6	-2.7	-.8	.9	2.5	4.7	7.6
4	21	125	0.653	-10.8	-9.9	-8.2	-9.0	-4.1	-6.8	-4.9	-3.6	-2.8	-1.8	-.2	1.5	3.1	4.4	6.9
8	22	160	0.835	-8.8	-7.6	-5.8	-3.7	-2.7	-3.7	-2.1	-3.5	-1.7	-2.0	1.0	1.4	3.3	3.3	5.1
•	23	200	1.044	-6.8	-5.5	-4.5	-3.1	-1.3	-3.3	-4.7	-3.1	-1.1	-.4	1.6	1.7	2.5	3.7	3.6
C	24	250	1.305	-1.9	-4.7	-5.4	-5.8	-1.9	-3.2	-1.3	-1.9	-.9	-.3	1.0	1.2	2.9	3.2	3.0
E	25	315	1.045	-6.5	-2.8	-4.5	-4.0	-.4	-1.5	1.4	3.8	2.0	-2.2	-1.3	-.2	-1.3	-.4	-.3
N	26	400	2.088	-8.2	-7.9	-2.5	-1.2	.8	4.6	3.4	.7	-4.2	-3.4	.4	-2.9	-6.2	-2.2	-3.2
T	27	500	2.611	-2.8	-1.5	-2.1	-.8	2.9	-.0	2.8	1.1	2.1	.2	-.2	-6.5	-4.9	-5.7	-2.0
R	28	630	3.289	-.7	.6	3.3	1.8	2.4	1.4	2.4	-.2	-.2	-5.6	-1.5	-4.1	-3.3	-2.6	-1.7
F	29	800	4.177	2.8	1.4	1.8	-2.0	.0	2.1	.8	-1.9	1.1	-1.7	-.9	-.5	-.9	-2.1	-3.0
R	30	1000	5.221	-2.3	3.5	1.2	.7	2.5	.5	-.9	.5	-.3	-3.7	-1.9	-1.2	-4.6	-3.6	-2.9
E	31	1250	6.526	-5.6	3.5	3.2	1.7	1.5	4.2	-.9	-1.3	-.5	-4.5	-3.6	-3.2	-5.6	-2.4	-2.8
Q	32	1600	8.358	4.4	2.7	4.4	.9	.5	3.5	-.5	-1.3	-1.4	-4.5	-4.4	-4.1	-4.4	-3.3	-3.6
U	33	2000	10.442	6.7	6.1	5.0	3.0	.8	-.0	-1.4	-1.8	-4.9	-6.2	-4.3	-6.1	-4.9	-5.8	-5.1
E	34	2500	13.053	5.8	4.5	5.1	4.1	1.0	-2.3	-.9	-1.6	-3.6	-4.8	-4.2	-6.8	-5.9	-5.7	-4.9
N	35	3150	16.446	3.5	4.6	5.4	2.5	1.6	-2.4	-1.6	-2.5	-2.4	-5.6	-4.8	-3.3	-6.3	-5.6	-5.5
C	36	4000	20.884	6.5	2.8	3.7	3.7	.5	-.6	-2.5	-1.3	-5.2	-5.6	-4.6	-5.1	-4.4	-5.4	-5.4
Y	37	5000	26.105	4.2	5.6	3.8	2.5	1.3	-1.9	-1.0	-1.5	-3.8	-7.8	-5.0	-5.8	-6.6	-4.6	-6.8
H	38	6300	32.893	3.5	2.6	3.5	3.8	-.1	-3.5	-2.8	-2.6	-4.4	-5.9	-4.8	-5.5	-5.5	-6.0	-6.9
E	39	8000	41.768	1.3	3.4	2.8	3.2	-1.1	-2.7	-2.9	-3.6	-3.6	-6.8	-5.1	-5.4	-5.5	-5.8	-7.8
R	40	10000	52.210	-.5	-.1	-.3	1.6	-.7	-6.5	-4.9	-6.3	-5.3	-7.5	-2.5	-1.5	-3.5	-5.3	-6.5
I																		
Z																		

Fig. 4. Sample page of 1/3-octave-band sound pressure level directivities at locations along 45.7-m radius polar arc and relative to surface-average 1/3-octave-band sound pressure level over surface of hemisphere.

VOLUME III NASA / GE Q U I E T E N G I N E C PAGE 39

CONFIGURATION - C O N T O U R E D I N L E T - NOMINAL NOZZLE
CONTOUR INLET / NO SPLITTERS, 94.7 CM SDOF INLET TMT
HDOF FAN FRAME, COMP. INLET / SCOTTFELT FAN EXH / SDOF CORE EXH

SOURCE - NASA QUIET ENGINE PROGRAM /GE/ NASA CR-121176 NAS3-12430
TEST SITE - PEEBLES,OHIO - 46.5 M ARC - 12.2 M POLE MICROPHONES
DESIGN POINT - THRUST=97.9 KN ; N1=4960 RPM ; BPR=5.0 ; 415 KG/S

TEST DATE : 04-11/72 M TOT = 365.1 KG/S ENGINE HT = 4.6 M GND SURFC : GRAVEL DISTANCE = 45.7 M RADIUS
RUN NUMBR : GEPC-90 EFF DIAM = 1.4 M SIGMA = 0.0 RYL/CM AMB TEMP = 25.0 DEG C
THRUST = 97.9 KN EFF VJ = 268.1 M/S ENG BPR = 5.0 MIC HT = 12.2 M REL HUMID = 70.0 PCT

D A T A S U M M A R Y I

	RND NUM	GMF /M2	STRHL NUMBR	PWL DB	45.7 M RADIUS PWL DB	45.7 M RADIUS PWL NORM DB	AWT PWL DB	AWT PWL NORM DB	SP AVG SPL, DB	SP AVG SPL NORM, DB	SPL DB	61.0 M SIDLNE SPLIPNLM DB	SPLIPNLTM DB	SPLIALM DB	SPLIOASM DB
1	17	50	0.261	135.1	-15.0	104.9	-42.9	93.9	-15.0	-17.4	80.8	80.8	80.8	80.8	80.8
/	18	63	0.329	132.6	-17.4	106.4	-41.4	91.5	-17.4	-18.8	80.7	80.7	80.7	80.7	80.7
3	19	80	0.418	131.3	-18.8	108.8	-39.0	90.1	-18.8		80.3	80.3	80.3	80.3	80.3
0	20	100	0.522	133.7	-16.4	114.6	-33.2	92.5	-16.4		81.9	81.9	81.9	81.9	81.9
A	21	125	0.653	136.4	-13.7	120.3	-27.5	95.2	-13.7		87.3	87.3	87.3	87.3	87.3
.	22	160	0.835	137.0	-13.1	123.6	-24.2	95.8	-13.1		90.7	90.7	90.7	90.7	90.7
C	23	200	1.044	134.8	-15.3	123.9	-23.9	93.6	-15.3		85.6	85.8	85.8	85.8	85.8
E	24	250	1.305	133.3	-16.7	124.7	-23.1	92.2	-16.7		87.8	87.8	87.8	87.8	87.8
N	25	315	1.645	136.6	-13.5	130.0	-17.8	95.4	-13.5		93.8	93.8	93.8	93.8	93.8
T	26	400	2.088	141.4	-8.7	136.6	-11.2	100.2	-8.7		100.5	100.5	100.5	100.5	100.5
E	27	500	2.611	142.1	-8.0	138.9	-8.9	100.9	-8.0		100.5	100.5	100.5	100.5	100.5
R	28	630	3.289	138.0	-12.1	136.1	-11.7	96.9	-12.1		96.1	96.1	96.1	96.1	96.1
F	29	800	4.177	136.3	-13.8	135.5	-12.3	95.1	-13.8		92.8	92.8	92.8	92.8	92.8
R	30	1000	5.221	137.1	-13.0	137.1	-10.7	96.0	-13.0		91.8	91.8	91.8	91.8	91.8
E	31	1250	6.526	135.9	-14.2	136.5	-11.3	94.7	-14.2		90.6	90.6	90.6	90.6	90.6
Q	32	1600	8.354	134.8	-15.3	135.8	-12.0	93.6	-15.3		89.9	89.9	89.9	89.9	89.9
U	33	2000	10.442	136.5	-13.6	137.7	-10.1	95.3	-13.6		90.6	90.6	90.6	90.6	90.6
E	34	2500	13.053	136.1	-14.0	137.4	-10.4	94.9	-14.0		90.6	90.6	90.6	90.6	90.6
N	35	3150	16.446	133.9	-16.2	135.1	-12.7	92.8	-16.2		87.8	87.8	87.8	87.8	87.8
C	36	4000	20.884	134.5	-15.6	135.5	-12.3	93.3	-15.6		87.3	87.3	87.3	87.3	87.3
Y	37	5000	26.105	133.4	-16.7	133.9	-13.9	92.2	-16.7		87.5	87.5	87.5	87.5	87.5
M	38	6300	32.893	133.3	-16.8	133.2	-14.6	92.1	-16.8		85.6	85.6	85.6	85.6	85.6
E	39	8000	41.768	132.6	-17.5	131.5	-16.3	91.4	-17.5		84.6	84.6	84.6	84.6	84.6
N	40	10000	52.210	132.6	-17.5	130.1	-17.7	91.4	-17.5		82.2	82.2	82.2	82.2	82.2
I															
Z															

OVERAL PWL = 150.1 DB
ACOUSTIC PWR = 1.021 KWATTS
ACOUSTIC EFFICIENCY = .0078 PRCNT
FORWARD PWL = 147.8 DB
REAR PWL = 146.2 DB

AWTD OVERAL PWL = 147.8 DB
AWTD ACOUSTIC PWR = .603 KWATTS
AWTD EFFICIENCY = .0046 PRCNT
FORWARD AWTD PWL = 146.5 DB
REAR AWTD PWL = 142.0 DB

SPACE AVG OASPL = 108.9 DB
ENGINE MECH PWR = 13.13 MEGAWATTS
PNLM = 115.6 DB AT 70.0 DEG
PNLTM = 115.6 DB AT 70.0 DEG
ALM = 103.8 DB AT 70.0 DEG

* SOUND POWER LEVEL, PWL - RE 10.0 ** -12 WATTS

Fig. 5 Sample page of calculated values of flat-weighted and A-weighted sound power levels, surface-average sound pressure levels, and 1/3-octave-band sound pressure levels on 61-m sideline at locations of maximum perceived noise level, maximum tone-corrected perceived noise level, and maximum A-weighted sound level. Also, acoustic power, jet-stream mechanical power, and acoustical efficiency.

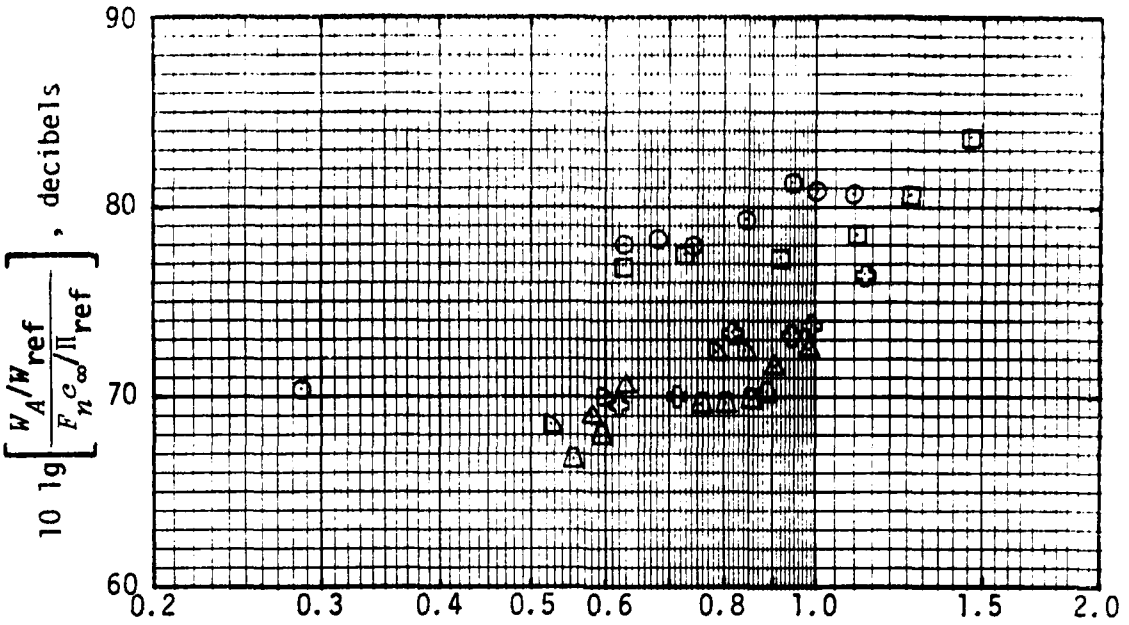

(1) ⊙ JT3D-3B, ⊡ JT8D-15, ✣ JT8D-209, ▷ CF6-6D, △ CF6-50C, ⧋ JT9D-70.

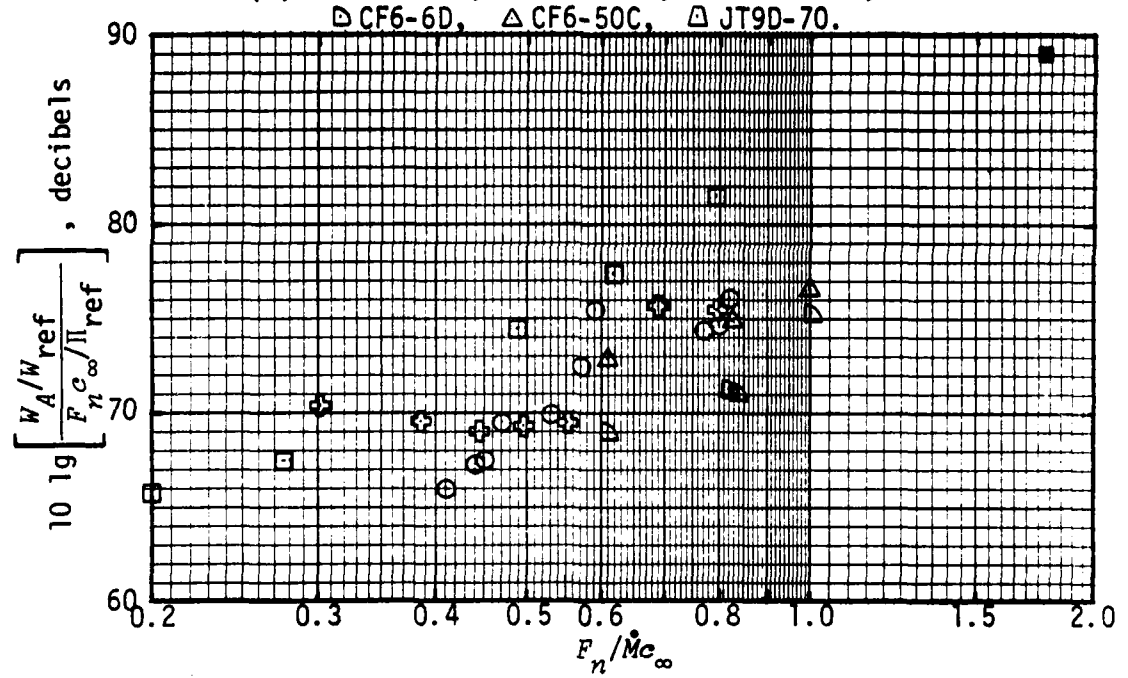

(2) ■ JT4A-3, ⊡ TF34-GE-100, ⊙ CF34, ✣ JT15D-1, △ JT8D-109 [Table 2(c)(1)], ▷ JT8D-109 [Table 2(c)(3)].

(a) Production engines, see Table 1 and Table 2(c) for configuration descriptions.

Fig. 6. Engine noise in terms of nondimensional A-weighted sound power.

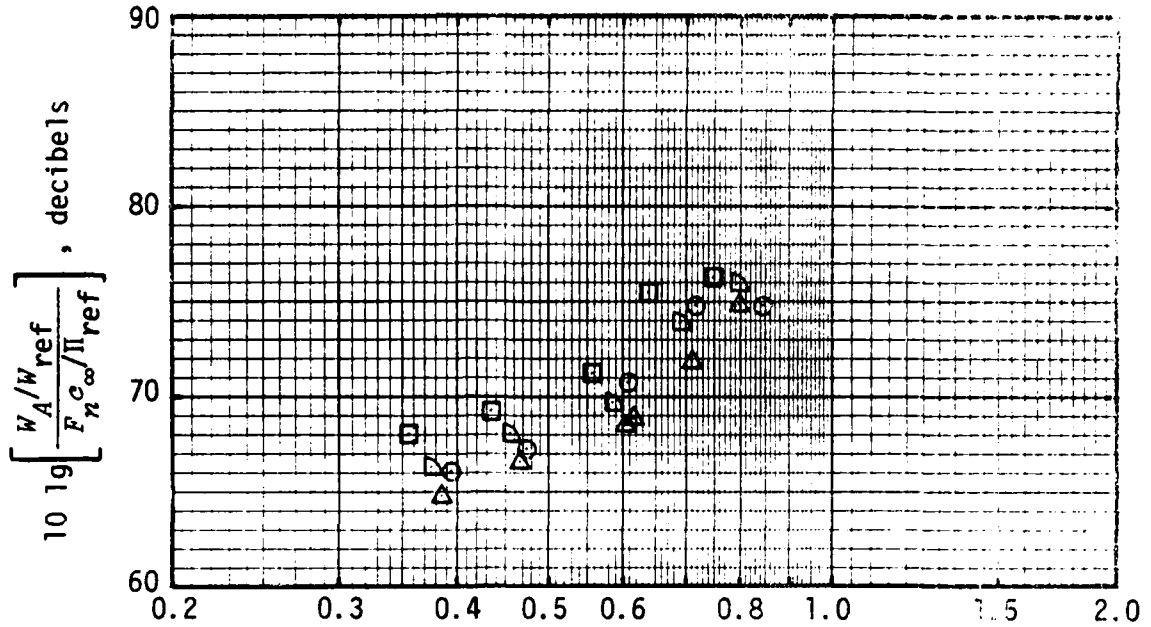

(b) QSRA/YF-102 [Table 2(d)].
- ⊡ confluent exhaust flow, large exit nozzle [2(d)(2)]
- ⊙ confluent exhaust flow, short core nozzle [2(d)(1)]
- ▷ separate exhaust flows, small core nozzle [2(d)(4)]
- △ confluent exhaust flow, small core nozzle [2(d)(3)]

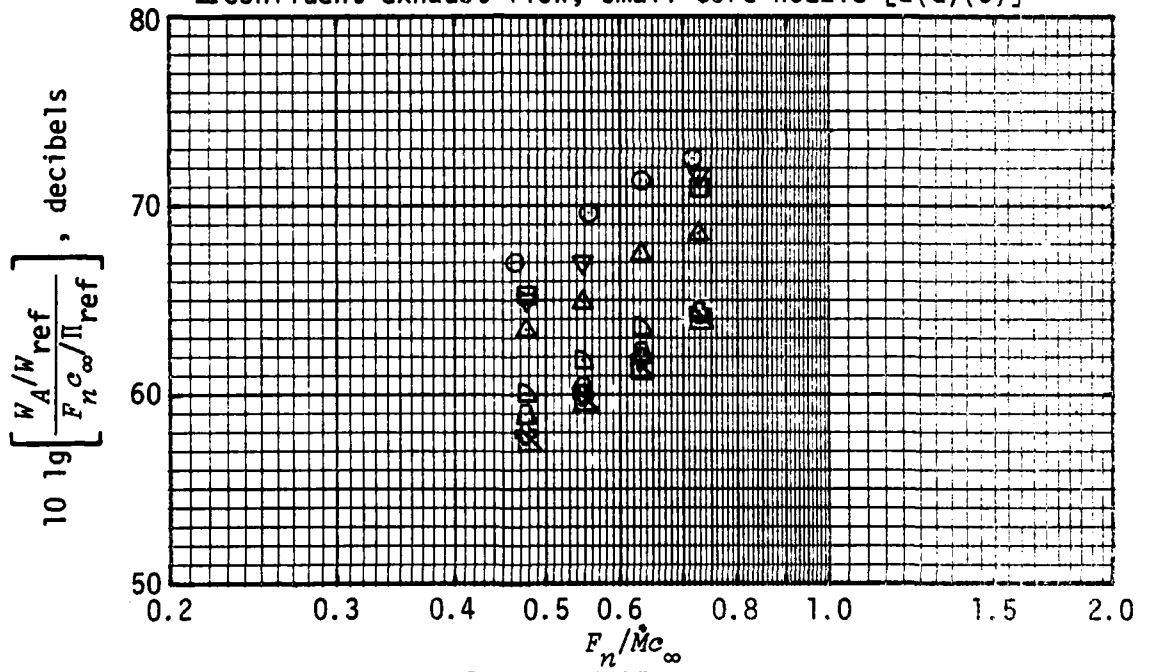

(c) Quiet Engine A [Table 2(a)].
- ⊙ inlet w/ simulated blow-in doors [2(a)(6)]
- ⊡ hardwall baseline ducts [2(a)(1)]
- ▽ [2(a)(5)], △ [2(a)(4)]
- ▷ one-ring inlet [2(a)(10)], ✣ three-ring inlet [2(a)(7)]
- ⏢ three-ring inlet + wrapped fan case [2(a)(8)]
- ◺ [2(a)(9)]

Fig. 6. Continued.

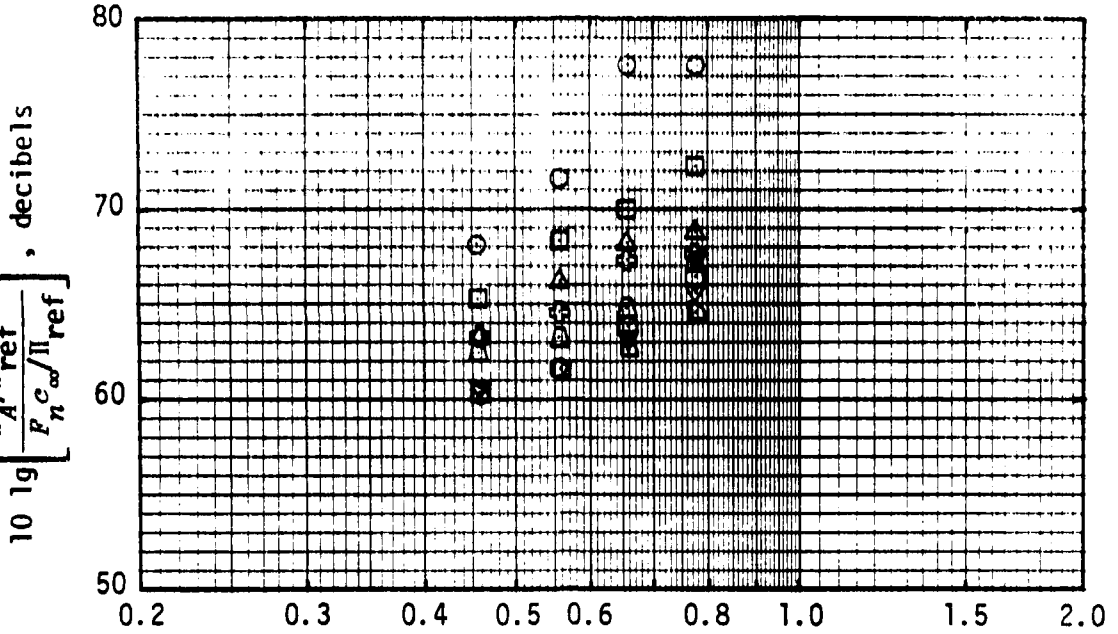

(1) ⊙ baseline [2(b)(1)], ⊡ 4-ring inlet, hardwall fan ducts [2(b)(3)]
△ 1-ring inlet [2(b)(9)], ✣ 2-ring inlet [2(b)(8)]
△ 3-ring inlet [2(b)(7)], ⊙ 4-ring inlet [2(b)(6)]
◁ 4-ring inlet, treated fan & turbine ducts, coplanar nozzles [2(b)(4)]
▷ 4-ring inlet, treated fan & turbine ducts, wrapped fan case [2(b)(2)]

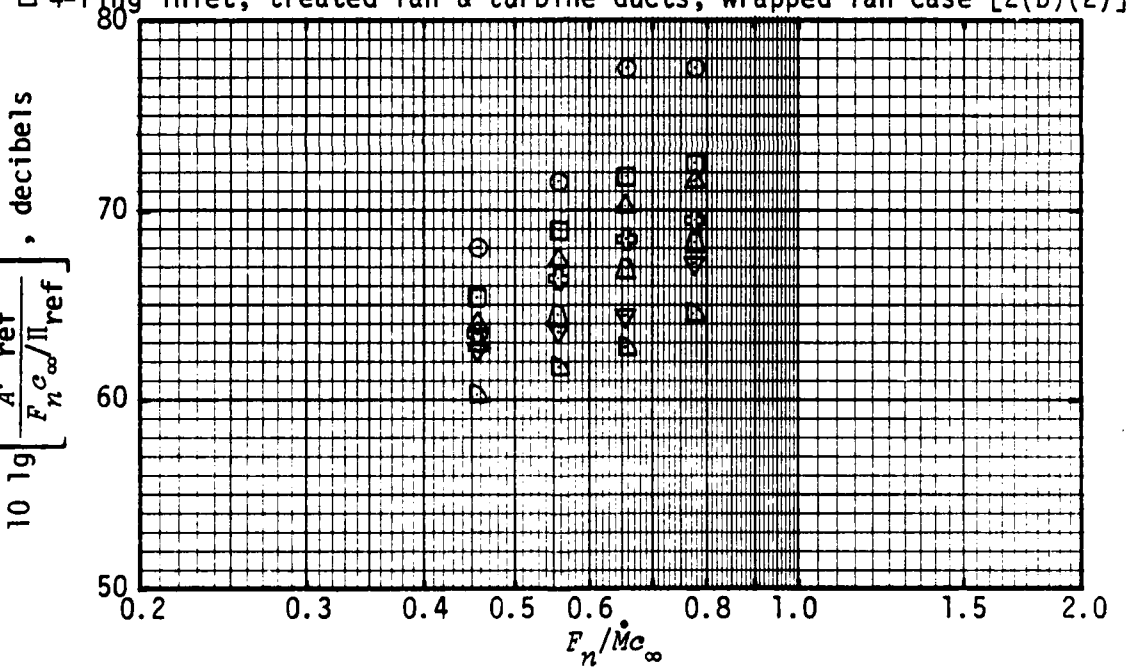

(2) ⊙ baseline [2(b)(1)], ⊡ SDOF on inlet cowl [2(b)(11)]
△ SDOF on long inlet cowl [2(b)(10)], ✣ 61 cm of thick SDOF [2(b)(12)]
△ 91 cm of thick SDOF on inlet cowl [2(b)(13)]
◁ 4-ring inlet, treated fan ducts, hardwall turbine ducts [2(b)(5)]
▷ 4-ring inlet, treated fan & turbine ducts, wrapped fan case [2(b)(2)]

(d) Quiet Engine C [Table 2(b)].

Fig. 6. Concluded.

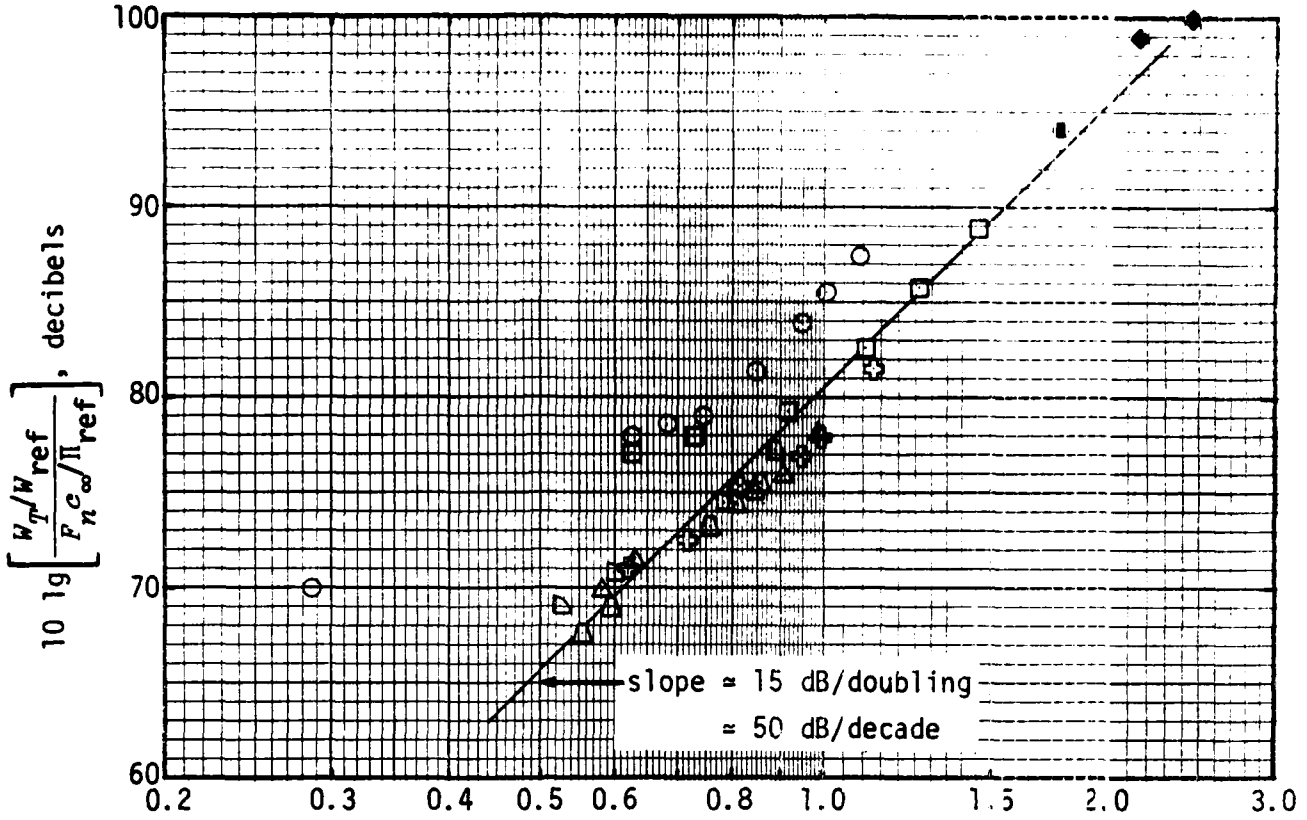

(1) ◆ OL-593, ■ JT4A-3, ⊙ JT3D-3B, ⊡ JT8D-15, ✣ JT8D-209, ▷ CF6-6D, △ CF6-50C, ▲ JT9D-70.

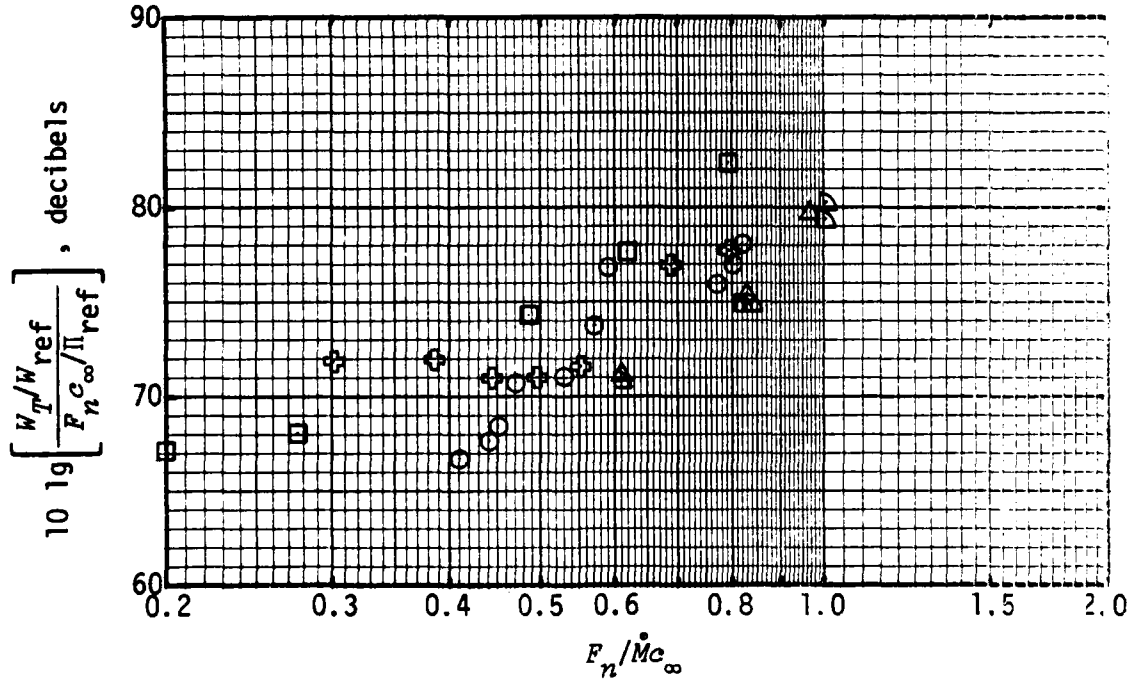

(2) ⊡ TF34-GE-100, ⊙ CF34, ✣ JT15D-1, △ JT8D-109 [Table 2(c)(1)], ▷ JT8D-109 [Table 2(c)(3)].

(a) Production engines, see Table 1 and Table 2(c) for configuration descriptions.

Fig. 7. Engine noise in terms of nondimensional flat (or unweighted) sound power.

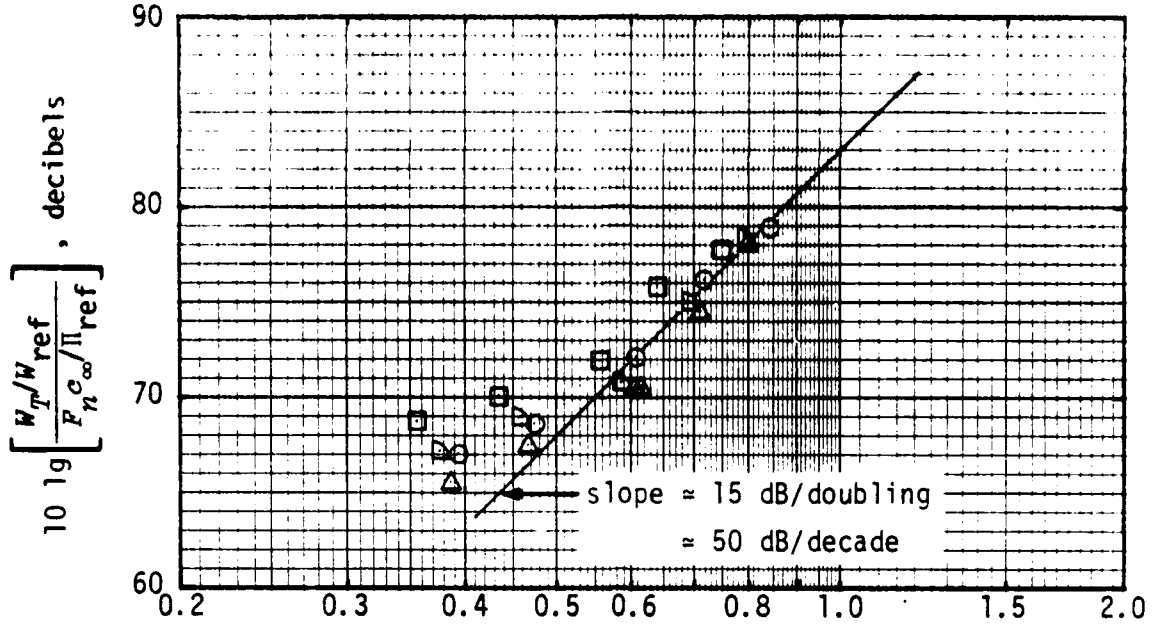

(b) QSRA/YF-102 [Table 2(d)].
- ⊡ confluent exhaust flow, large exit nozzle [2(d)(2)]
- ⊙ confluent exhaust flow, short core nozzle [2(d)(1)]
- ◺ separate exhaust flows, small core nozzle [2(d)(4)]
- △ confluent exhaust flow, small core nozzle [2(d)(3)]

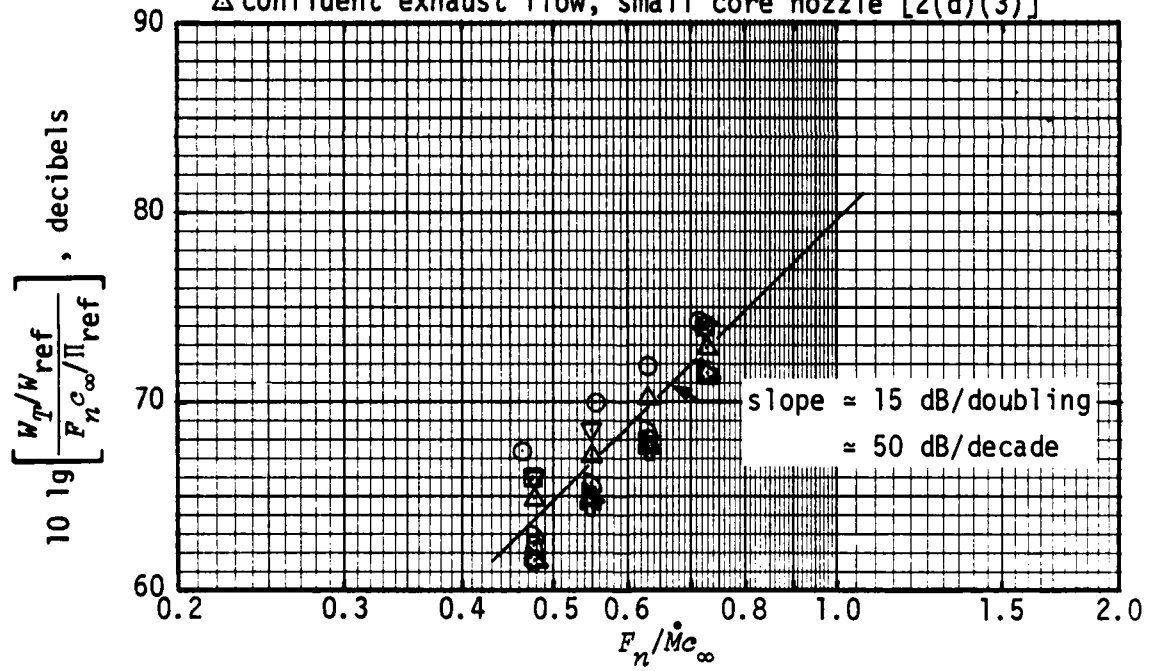

(c) Quiet Engine A [Table 2(a)].
- ⊙ inlet w/ simulated blow-in doors [2(a)(6)]
- ⊡ hardwall baseline ducts [2(a)(1)]
- ▽ [2(a)(5)], △ [2(a)(4)]
- ◺ one-ring inlet [2(a)(10)], ✣ three-ring inlet [2(a)(7)]
- ◬ three-ring inlet + wrapped fan case [2(a)(8)]
- ◺ [2(a)(9)]

Fig. 7. Continued.

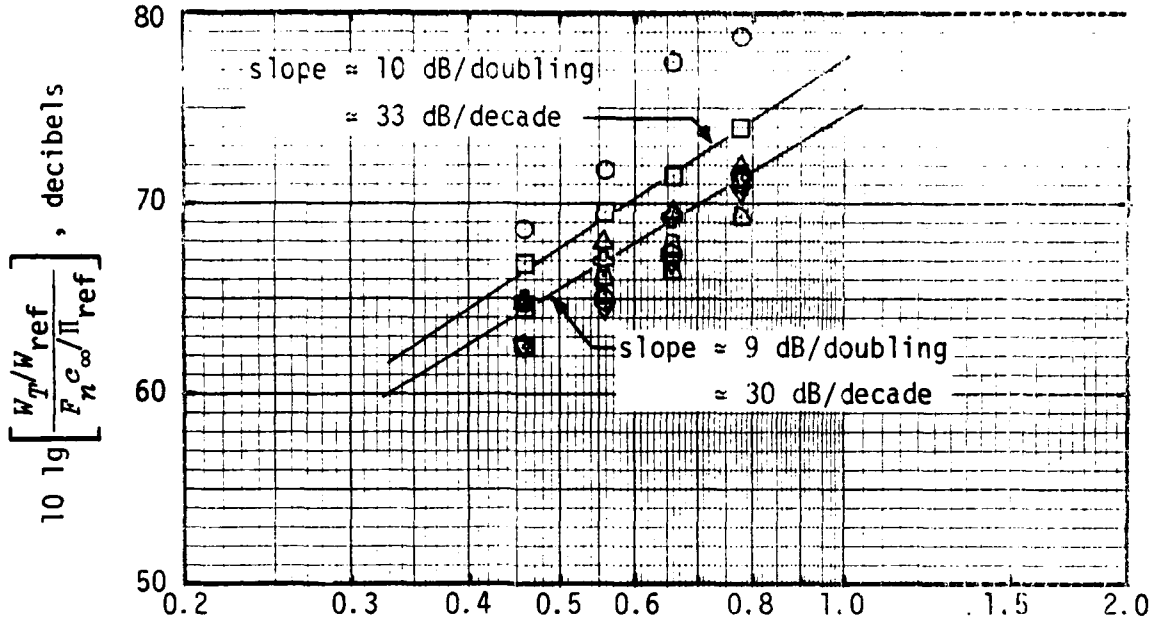

(1) ⊙ baseline [2(b)(1)], ⊡ 4-ring inlet, hardwall fan ducts [2(b)(3)]
△ 1-ring inlet [2(b)(9)], ✣ 2-ring inlet [2(b)(8)]
⊡ 3-ring inlet [2(b)(7)], ⊙ 4-ring inlet [2(b)(6)]
▽ 4-ring inlet, treated fan & turbine ducts, coplanar nozzles [2(b)(4)]
▷ 4-ring inlet, treated fan & turbine ducts, wrapped fan case [2(b)(2)]

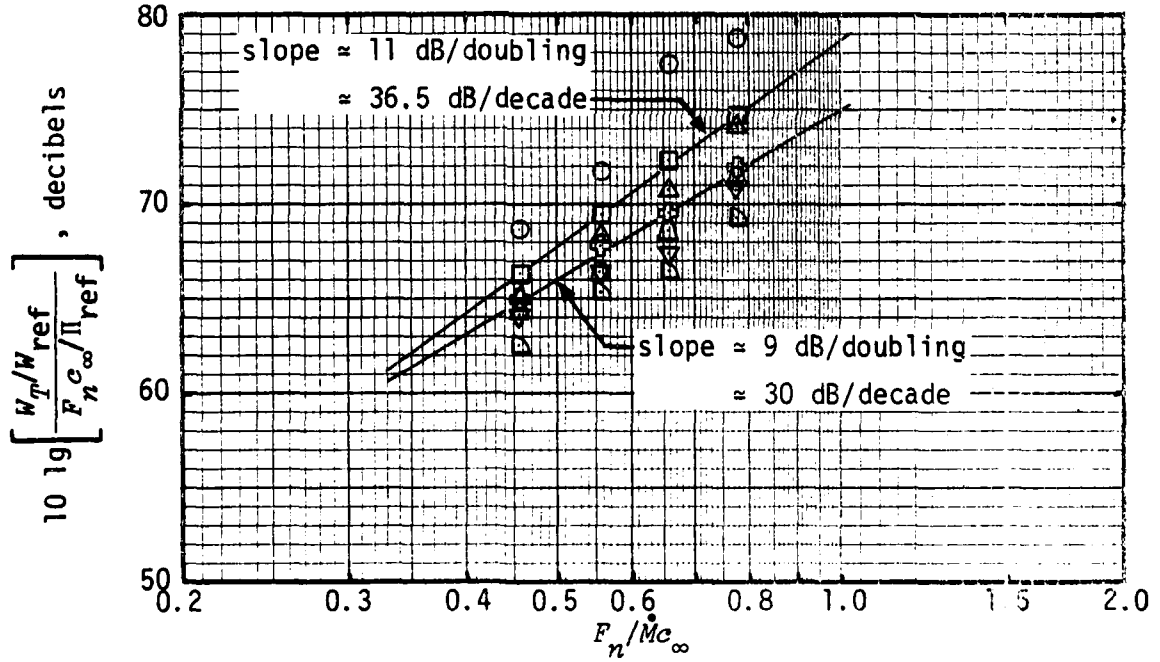

(2) ⊙ baseline [2(b)(1)], ⊡ SDOF on inlet cowl [2(b)(11)]
△ SDOF on long inlet cowl [2(b)(10)], ✣ 61 cm of thick SDOF [2(b)(12)]
⊡ 91 cm of thick SDOF on inlet cowl [2(b)(13)]
▽ 4-ring inlet, treated fan ducts, hardwall turbine ducts [2(b)(5)]
▷ 4-ring inlet, treated fan & turbine ducts, wrapped fan case [2(b)(2)]

(d) Quiet Engine C [Table 2(b)].

Fig. 7. Concluded.

APPENDIX

REFERENCES FOR EFFECTS OF FORWARD MOTION ON NOISE FROM JET ENGINES

1. Bushell, K. W. Measurement and Prediction of Jet Noise in Flight. AIAA Paper 75-461, March 1975.

2. Lowrie, B. W. Simulation of Flight Effects on Aero Engine Fan Noise. AIAA Paper 75-463, March 1975.

3. Roundhill, J. P. and Schaut, L. W. Model and Full Scale Test Results Relating to Fan Noise In-Flight Effects. AIAA Paper 75-465, March 1975.

4. Hanson, D. B. Measurements of Static Inlet Turbulence. AIAA Paper 75-467, March 1975.

5. Brooks, J. R. and Woodrow, R. J. The Effects of Forward Speed on a Number of Turbojet Exhaust Silencers. AIAA Paper 75-506, March 1975.

6. Crighton, D. G., Ffowcs Williams, J. E. and Cheesman, I. C. The Outlook for Simulation of Forward Velocity Effects on Aircraft Noise. AIAA Paper 76-530, July 1976.

7. Ribner, H. S. (ed.) Workshop on Effects of Forward Velocity on Jet Noise. NASA Langley Research Center, January 15 and 16, 1976.

8. Clapper, W. S., et al. High Velocity Jet Noise Source Location and Reduction, Task 4 – Development/Evaluation of Techniques for 'Inflight' Investigation. FAA-RD-76-79, IV, February 22, 1977.

9. Chun, K. S., Berman, C. H. and Cowan, S. J. Effects of Motion on Jet Exhaust Noise from Aircraft. NASA CR-2701, June 1976.

10. Strout, F. G. Flight Effects on Noise Generated by the JT8D-17 Engine in a Quiet Nacelle and a Conventional Nacelle as Measured in the NASA-Ames 40 x 80 Foot Wind Tunnel. NASA CR-137797, January 1976.

11. Plumblee, H. E. (ed.) Effects of Forward Velocity on Turbulent Jet Mixing Noise. NASA CR-2702, July 1976.

12. Williams, J. Problems of Noise Measurement in Ground Based Facilities With Forward Motion Simulation (Noise Model Testing). AGARD AR-83, Appendix 4, pp. 59-100, (1975).

13. Feiler, C. E. and Merriman, J. E. Effects of Forward Velocity and Acoustic Treatment on Inlet Fan Noise. AIAA Paper 74-946, August 1974.

14. Wilby, J. F. and Piersol, A. G. Coherence and Phase Techniques Applied to Wind Tunnel Acoustics. AIAA Paper 77-1306, October 1977.

15. Feiler, C. E. and Groeneweg, J. F. Summary of Forward Velocity Effects on Fan Noise. AIAA Paper 77-1319, October 1977.

16. Brooks, J. R. Flight Noise Studies on a Turbojet Using Microphones Mounted on a 450-ft Tower. AIAA Paper 77-1325, October 1977.

17. Low, J. K. C. Effects of Forward Motion on Jet and Core Noise. AIAA Paper 77-1330, October 1977.

18. Heidmann, J. F. and Dietrich. D. A. Effects of Simulated Flight on Fan Noise Suppression. AIAA Paper 77-1334, October 1977.

19. Shaw, L. M., Woodward, R. P. and Glaser, F. W. Inlet Turbulence and Fan Noise Measured in an Anechoic Wind Tunnel and Statically With an Inlet Flow Control Device. AIAA Paper 77-1345, October 1977.

20. Blankenship, G. L. Effect of Forward Motion on Turbomachinery Noise. AIAA Paper 77-1346. October 1977.

21. deBelleval, J-F., Chen, C. Y., and Perulli, M. Investigation of In-Flight Jet Noise Based on Measurements in an Anechoic Wind Tunnel. Sixieme Congres International sur l'Instrumentation dans les Installations de Simulation Aerospatiale. Ottawa, September 22-24, 1975.

22. Bongrand, J., Julienne, A. and Perulli, M. Soufflerie Anechoique pour la Simuation de l'Effect de Vol Sun Les Bruits des Jets (An Anechoic Wind Tunnel for the Simulation of the Effects of Forward Velocity on Jet Noise). L'Aeronautique et l'Astronautique, 1976, pp. 40-46.

23. Clark, B. J., Heidmann, M. F. and Kreim, W. J. Macroscopic Study of Time Unsteady Noise of An Aircraft Engine During Static Tests. NASA TMX-73556, November 1976.

24. Heidmann, M. F. and Clark, B. J. Flight Effects on Predicted Fan Fly-By Noise. NASA TM-73798, December 1977.

25. Woodward, R. P., Wazyniak, J. A., Shaw, L. M. and McKinnon, J. J. Effectiveness of an Inlet Flow Turbulence Control Device to Simulate Flight Fan Noise in an Anechoic Chamber. NASA TM-73855, December 1977.

26. Morfey, C. L. and Tester, B. J. Noise Measurements in a Free Jet, Flight Simulation Facility: Shear Layer Refraction and Static-to-Flight Corrections. AIAA Paper 76-531, July 1976.

27. Clapper, W. S., Banerian, G. and Mani, R. Development of a Technique for Inflight Jet Noise Simulation – Parts I and II. AIAA Paper 76-532, July 1976.

28. deBelleval, J-F., Candel, S. M., Julienne, A. and Perulli, M. Analysis of Problems Posed by Simulation of Flight Effects in Anechoic Open Wind Tunnels. AIAA Paper 76-533, July 1976.

29. Tanna, H. K. and Morris, P. J. Inflight Simulation Experiments on Turbulent Jet Mixing Noise. AIAA Paper 76-554, July 1976.

30. Cocking, B. J. The Prediction of Flight Effects on Jet Noise. AIAA Paper 76-555, July 1976.

31. Strout, F. G. and Atencio, A. Jr. Flight Effects on JT8D Engine Jet Noise as Measured in the 40 x 80 Foot Wind Tunnel. AIAA Paper 76-556, July 1976.

32. Drevet, P., Duponchel, J. P. and Jaques, J. R. Effect of Flight on the Noise from a Convergent Nozzle as Observed on the Bertin Aerotrain. AIAA Paper 76-557, July 1976.

33. Sarohia, V., Parthasarathy, S. P. and Massier, P. F. Effects of External Boundary Layer Flow on Jet Noise in Flight. AIAA Paper 76-558, July 1976.

34. deBelleval, J-F., Leuchter, O. and Perulli, M. Simulation of Flight Effects on the Structure of Jet Mixing Layers for Acoustical Applications. AIAA Paper 76-559, July 1976.

35. Merriman, J. E., Low, K. C. and Yee, P. M. Forward Motion and Installation Effects on Engine Noise. AIAA Paper 76-584, July 1976.

36. Stone, J. R., Miles, J. H. and Sargent, N. B. Effects of Forward Velocity on Noise for a J85 Turbojet Engine With Multitube Suppressor From Wind Tunnel and Flight Tests. NASA TMX-73542, November 1976.

37. von Glahn, U. and Goodykoontz, J. Forward Velocity Effects on Jet Noise With Dominant Internal Noise Source. NASA TMX-71438, November 1976.

38. Stone, J. R. Flight Effects on Exhaust Noise for Turbojet and Turbofan Engines – Comparison of Experimental Data With Prediction. NASA TMX-73552, November 1976.

39. Atencio, A., Jr. and Soderman, P. T. Comparison of Wind Tunnel and Flyover Noise Measurements of the YOV-10A STOL Aircraft. NASA TMX-62166, June 1972.

40. Atencio, A., Jr., Kirk, J. V., Soderman, P. T. and Hall, L. P. Comparison of Flight and Wind Tunnel Measurements of Jet Noise for the XV-5B Aircraft. NASA TMX-62182, October 1971.

41. Ahtye, W. F. and Kojima, G. K. Correlation Microphone for Measuring Airframe Noise in Large-Scale Wind Tunnels. AIAA Paper 76-553, July 1976.

42. Merriman, J. E. and Good, R. C. Effect of Forward Motion on Fan Noise. AIAA Paper 75-464, March 1975.

43. Stone, J. R. Prediction of In-Flight Exhaust Noise for Turbojet and Turbofan Engines. Noise Control Engineering, 10, pp. 40-46, January/February 1978.

REFERENCES

1. Alan H. Marsh: Study of noise-certification standards for aircraft engines, Volume 1: Noise-control technology for turbofan engines. FAA Contractor Report FAA-EE-82-11, Vol. 1 (June 1983).

2. Alan H. Marsh: Study of noise-certification standards for aircraft engines, Volume 2: Procedures for measuring farfield sound pressure levels around an outdoor jet-engine test stand. FAA Contractor Report FAA-EE-82-11, Vol. 2 (June 1983).

3. American National Standard Precision methods for the determination of sound power levels of noise sources in anechoic and hemi-anechoic rooms. ANSI S1.35-1979.

4. Acoustics – Determination of sound power levels of noise sources – Precision methods for anechoic and semi-anechoic rooms. International Standard ISO 3745-1977.

5. Marcus F. Heidmann and Charles E. Feiler: Noise comparisons from full-scale fan tests at NASA Lewis Research Center. AIAA Paper No. 73-1017 (October 1973).

6. James E. McCune and Jack L. Kerrebrock: Noise from aircraft turbomachinery. *Annual Review of Fluid Mechanics*, Vol. 5, 281-299 (1973).

7. Unpublished JT15D-1 engine noise data. NASA Lewis Research Center.

8. Unpublished TF34-GE-100 engine test stand far field noise data. U.S. Air Force, Aerospace Medical Research Center.

9. Unpublished CF34 engine noise data. General Electric Company.

10. Unpublished JT4A-3 engine noise data. Douglas Aircraft Company, McDonnell Douglas Corporation.

11. J. Kenneth Manhart, D. A. Campbell, C. A. Henry, and E. M. Lowder: Investigation of DC-8 nacelle modifications to reduce fan-compressor noise in airport communities. Part III – Static tests of noise-suppressor configurations. NASA Contractor Report CR-1707 (December 1970).

12. Unpublished data for JT8D-15, JT8D-209, and JT9D-70 engines, Pratt & Whitney Group, United Technologies Corporation.

13. Unpublished CF6-6D and CF6-50C engine noise data. General Electric Company.

14. Unpublished Olympus 593 engine noise data. Rolls Royce Limited (Bristol).

15. S. B. Kazin and J. E. Paas: NASA/GE Quiet Engine "A" Acoustic Test Results, NASA CR-121175, October 1973.

16. S. B. Kazin and J. E. Paas: NASA/GE Quiet Engine "C" Acoustic Test Results, NASA CR-121176, April 1974.

17. E. A. Burdsall, F. P. Brocher, V. M. Scaramella: Results of Acoustic Testing of the JT8D-109 Refan Engines, NASA CR-134875, November 1975.

18. Unpublished Memorandum from B. J. Clark to M. F. Valerino (NASA Lewis Research Center), LeRC Acoustic Test Results for YF102 Engine, Effects of Various Exhaust Nozzle Geometries, April 15, 1976.

19. J. Atvars, G. C. Paynter, D. Q. Walker, and C. F. Wintermeyer: Development of Acoustically Lined Ejector Technology for Multitube Jet Noise Suppressor Nozzles by Model and Engine Tests over a Wide Range of Jet Pressure Ratios and Temperatures, NASA CR-2382 (Contract NAS3-15570), April 1974.

20. M. T. Moore and V. L. Doyle: Evaluation of the In-Flight Noise Signature of a 32-Chute Suppressor Nozzle, Acoustic Data Report, NASA CR-152076, November 1977.

21. Frank G. Strout: Flight Effects on Noise Generated by the JT8D-17 Engine in a Quiet Nacelle as Measured in the NASA-Ames 40 by 80-Foot Wind Tunnel, NASA CR-137797, January 1976.

22. Frank G. Strout: Flight Effects on Noise Generated by the JT8D Engine With Inverted Primary/Fan Flow as Measured in the NASA-Ames 40 by 80-Foot Wind Tunnel, NASA CR-2996, June 1978.

23. D. L. Stimpert: Quiet Clean Short-Haul Experimental Engine (QCSEE) Under-the-Wing (UTW) Composite Nacelle Test Report, Volume II – Acoustic Performance, NASA CR-159472, November 1979.

24. D. L. Stimpert: Quiet Clean Short-Haul Experimental Engine (QCSEE) Under-the-Wing (UTW) Composite Nacelle Test Report, Appendix B – Acoustic Data, General Electric Co. Report R78AEG576, November 1979.

25. D. L. Stimpert: Quiet Clean Short Haul Experimental Engine (QCSEE) Over-the-Wing (OTW) Composite Nacelle Test Report, Volume IV Acoustic Performance, NASA CR-135326, February 1979.

26. D. L. Stimpert: Quiet Clean Short Haul Experimental Engine (QCSEE) Over-the-Wing (OTW) Propulsion System Test Report, Appendix B – Acoustic Data, General Electric Co. Report R77AEG478, April 1979.

27. Leif E. Hoglund: Static Source Locations for Four Nozzles Mounted on a J-85 Engine, Beam Engineering, Inc. Final Report for NASA Contract NAS2-9399, January 1979.

28. V. L. Doyle and M. T. Moore: Core Noise Investigation of the CF6-50 Turbofan Engine – Final Report, NASA CR-159749, January 1980.

29. V. L. Doyle: Core Noise Investigation of the CF6-50 Turbofan Engine – Data Report, NASA CR-159598, January 1980.

END

FILMED

3-84

DTIC